BULGARIAN ACADEMY OF SCIENCES

INSTITUTE OF MICROBIOLOGY

“STEPHAN ANGELOFF”

Monika Nikolaeva Todorova

MODULATION OF LONGEVITY-ASSOCIATED MECHANISMS IN *CAENORHABDITIS ELEGANS* THROUGH BIOLOGICALLY ACTIVE COMPOUNDS

SUMMARY

Of a dissertation for the award of the educational and scientific degree “Doctor” in the professional field 5. Technical Sciences, scientific specialty 5.11. Biotechnologies (Technology of Biologically Active Substances)

Scientific supervisor: Prof. Dr. Milen I. Georgiev

Plovdiv, 2026

The dissertation comprises 161 pages and is illustrated with 31 figures and 12 tables. A total of 271 literature sources are cited.

The dissertation has been approved and scheduled for defense by the National Scientific Seminar in “Applied Microbiology and Microbial Biotechnologies” at the Institute of Microbiology “Stefan Angelov”, Bulgarian Academy of Sciences. The seminar session was held on April 21, 2026.

The PhD candidate was granted the right to defend the dissertation by Order No. I-184/17.12.2024, issued by the Director of the Institute of Microbiology, BAS, prof. Penka Petrova, DSc.

Members of the scientific jury:

Assoc. Prof. Dr. Nikolina Mihaylova

Prof. Dr. Milka Mileva

Prof. Dr. Milena Georgieva, DSc

Prof. Dr. Albert Krastanov, DSc

Prof. Dr. Petko Denev

The dissertation defense will take place at ..... from ..... hours in the seminar hall of the Institute of Microbiology “Stephan Angeloff” – BAS (IMikB), Sofia, Bulgaria.

The defense materials are available at IMikB – BAS and are published on the IMikB – BAS website.

Content:

Abbreviations and symbols:

$_{\Delta}\Psi m$ – mitochondrial membrane potential

a.u. –arbitrary units

ADAPT-232 – ADAPT® Energy Boost

AKT – protein kinase B

AMPK – adenosine monophosphate-activated protein kinase

APOE – apolipoprotein E

ATP – adenosine triphosphate

cDNA – complementary DNA

CI – chemotaxis index

CRP – C-reactive protein

DMSO – dimethyl sulfoxide

ER – endoplasmic reticulum

fmo-2 – flavin-containing monooxygenase 2

FOXO – Forkhead box O

GH – growth hormone

HIF-1 – hypoxia-inducible factor 1

HSF-1 – heat shock factor 1

HSPs – heat shock proteins

IGF-1 – insulin-like growth factor 1

IGF-1R – IGF-1 receptor

IIS – insulin/insulin-like signaling

IL – interleukin

iPSC – induced pluripotent stem cells

JAK – Janus kinase

JNK – c-Jun N-terminal kinase

L1 – larval stage 1

L2 – larval stage 2

L3 – larval stage 3

L4 – larval stage 4

MAPK – mitogen-activated protein kinase

MEK – MAPK/ERK kinase

mTOR – mechanistic target of rapamycinm

mTORC1 – mechanistic target of rapamycin complex 1

MTT – 3-(4,5-dimethylthiazol-2-yl)-2,5-diphenyltetrazolium bromide

MVG – MitoView Green

N2 – wild-type *C. elegans*

NAD^+ – nicotinamide adenine dinucleotide

NF-κB – nuclear factor kappa B

NGM – nematode growth medium

NLRP3 – NLR family pyrin domain containing 3

NMN – nicotinamide mononucleotide

NRF2 – nuclear factor erythroid 2-related factor 2

One-way ANOVA – one-way analysis of variance

PGC-1α – peroxisome proliferator-activated receptor gamma coactivator 1-alpha

PGJ – lyophilized *P. granatum* juice

PGL – *P. granatum* leaf extract

PI3K – phosphoinositide 3-kinase

ROS – reactive oxygen species

RT-qPCR – real-time quantitative polymerase chain reaction

SASP – senescence-associated secretory phenotype

sek-1 – dual-specificity mitogen-activated protein kinase kinase 1

SEM – standard error of the mean

SIRTs – NAD^+-dependent histone deacetylases (sirtuins)

TFEB – transcription factor EB

TMRE – tetramethylrhodamine ethyl ester

UPR – unfolded protein response

I. INTRODUCTION

Aging is a complex and multifactorial biological process characterized by the gradual accumulation of molecular and cellular damage, functional decline of the organism, and an increased risk of disease onset (Argentieri et al., 2024; Cohen et al., 2022; Shen et al., 2024). The interplay between genetic, epigenetic, and environmental factors determines both lifespan and the dynamics of age-related changes that accumulate at the molecular, cellular, and physiological levels (Fuellen et al., 2019; López-Otín et al., 2013, 2023).

Over the past century, life expectancy has increased significantly due to advances in medicine, pharmaceuticals, and technology. However, this has been accompanied by a progressive aging of the population, which is emerging as one of the most significant challenges facing modern society (Chen et al., 2018; Guo et al., 2022). The proportion of individuals aged 65 years and older is increasing both in the European Union and globally, with projections indicating further growth in the coming decades – while in 2021 one in ten individuals was aged 65 or older, this is expected to rise to one in six by mid-century (Chang et al., 2019). Despite increased lifespan, healthspan does not increase proportionally, with approximately 16–20% of life spent in poor health due to chronic age-related diseases (Chen et al., 2018, 2025).

Aging affects sensory, motor, and cognitive functions and represents a major risk factor for the development of neurodegenerative diseases (e.g., Alzheimer’s disease and Parkinson’s disease), cardiovascular and metabolic disorders, as well as certain types of neoplasms. At the core of these pathologies lies the accumulation of molecular damage and disruption of cellular homeostasis (Tyshkovskiy et al., 2023). Over the past decades, key molecular and cellular mechanisms of aging have been identified, including loss of proteostasis, mitochondrial dysfunction, chronic inflammation, epigenetic alterations, reduced repair capacity, and metabolic dysregulation (López-Otín et al., 2013, 2023). These discoveries have laid the foundation for the development of interventions aimed at modulating signaling pathways involved in the regulation of aging processes.

In contemporary biomedical science, aging is increasingly recognized as a primary risk factor and underlying cause of most chronic non-communicable diseases (Chang et al., 2019; Guo et al., 2022). Accumulating experimental and clinical evidence supports the concept that slowing aging may not only reduce the risk of multimorbidity but also extend the period of healthspan (Fahy et al., 2019; Fong et al., 2024; Kok et al., 2025; Liu et al., 2025). Therefore,

modern science faces the challenge of identifying innovative strategies to delay biological aging, extend healthspan, and reduce the burden of age-related pathologies.

Among the promising approaches for modulating ageing is the utilization of plant extracts and functional foods rich in phytochemicals (Fahey et al., 2021; Guo et al., 2022; Longo and Anderson, 2022). Natural products represent a valuable source of secondary metabolites with well-documented health benefits, attributable to their anti-inflammatory, neuroprotective, and metabolism-regulating properties (Atanasov et al., 2021; Li et al., 2024). Collectively, these characteristics make them promising candidates for promoting healthy longevity.

The investigation of ageing mechanisms and the effects of potential geroprotective interventions requires the use of appropriate model organisms. The nematode *Caenorhabditis elegans* is a well-established experimental model in ageing and longevity research due to its short lifespan, fully sequenced and well-characterized genome, and the presence of evolutionarily conserved signaling pathways shared with higher organisms, including humans (Lin et al., 2023; Mack et al., 2018). These features make it particularly suitable for the preclinical evaluation of natural products in relation to lifespan, stress resistance, metabolic homeostasis, and mitochondrial function.

Based on the above considerations, the present dissertation aims to investigate the potential of selected natural products, including plant extracts, biologically active substances, and functional foods, to modulate key processes associated with ageing, using *Caenorhabditis elegans* as a model system. By integrating phenotypic, molecular, and functional analyses, this research seeks to contribute to a more comprehensive understanding of the mechanisms through which natural products may promote healthy ageing and to provide a foundation for the development of novel geroprotective strategies.

II. AIM AND OBJECTIVES

1. Aim

The present dissertation aims to evaluate the geroprotective potential of selected natural products on key physiological and molecular markers of ageing. Central to this work is the development and validation of an integrated preclinical experimental platform for longevity assessment, based on the model organism *Caenorhabditis elegans*, which is characterized by a high degree of genetic homology with humans and enables the systematic investigation of the biological effects of natural products interventions.

Within the scope of this dissertation, the flavonoid icariin, leaf extract and juice of *Punica granatum*, as well as a combined product containing a standardized mixture of adaptogenic plant extracts were investigated. Their effects on lifespan, lipid metabolism, resistance to oxidative and thermal stress, as well as on the expression of genes and proteins associated with the regulation of ageing processes were assessed. The experimental strategy employed is summarized in Figure 1.

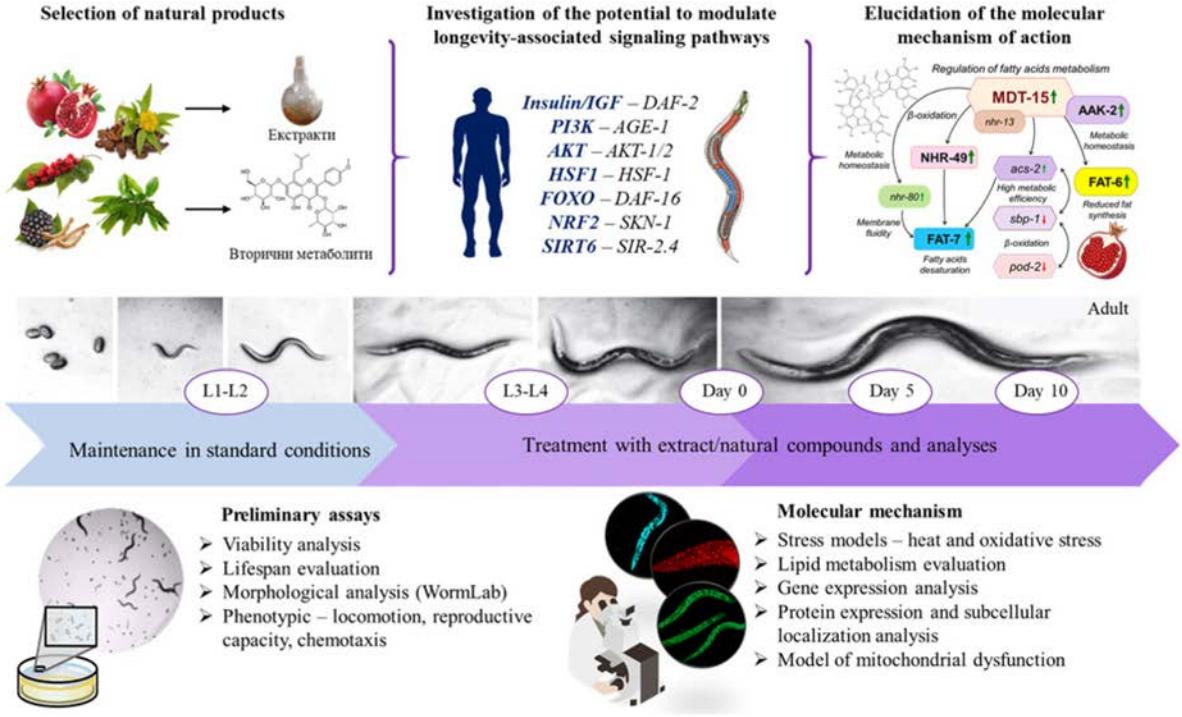

Fugure 1. Experimental strategy employed in the present dissertation.

2. Objectives

3a To achieve the aim of the present dissertation, the following objectives were defined:

2.1. Selection of plant species and secondary metabolites with potential effects on the lifespan of *C. elegans*.

2.2. Implementation of methodologies for the cultivation of *C. elegans*, characterization of physiological processes, and determination of lifespan and survival under conditions of induced stress of different origins.

2.3. Adaptation of methods for monitoring the nuclear translocation of selected proteins in *C. elegans*.

2.4. Development of a model of mitochondrial dysfunction in *C. elegans* and integration of methods for assessing mitochondrial dynamics.

2.5. Determination of the effects of icariin on lifespan, stress resistance, and basal lipid metabolism in *C. elegans*, and elucidation of its mechanism of action.

2.6. Metabolic profiling of leaf extract from *Punica granatum* L. (pomegranate), investigation of its effects on lifespan, stress resistance, and basal lipid metabolism in *C. elegans*, and elucidation of the underlying molecular mechanism.

2.7. Evaluation of the potential of *P. granatum* fruit juice to improve lifespan and healthspan in *C. elegans*.

2.8. Investigation of the potential of a standardized combined product containing extracts from adaptogenic medicinal plants to extend lifespan in *C. elegans*.

III. MATERIALS AND METHODS

1. Materials

1.1. Chemicals, reagents, pure compounds, and plant materials

Nematode growth medium (NGM; #MBS652667) was purchased from MyBiosource Inc. (San Diego, CA, USA). Luria–Bertani (LB) broth (Lennox modification; #L3022), mounting medium for histological preparations (#F6182), Nile Red solution (NR; #72485), agar (#05039), M9 buffer (#M6030), DMSO, isopropanol, Bradford reagent, radioimmunoprecipitation assay (RIPA) lysis buffer, protease and phosphatase inhibitor cocktail (#PPC1010), 3-(4,5-dimethylthiazol-2-yl)-2,5-diphenyltetrazolium bromide (MTT; #M2128), sodium hydroxide, methyl viologen (≥98% purity), and all other standard reagents were obtained from Sigma-Aldrich Co. (St. Louis, MO, USA).All reagents and consumables for RNA isolation, gel electrophoresis, and RT-qPCR analysis were purchased from Bio-Rad (Hercules, CA, USA). Deuterated methanol and water were supplied by Deutero GmbH (Kastellaun, Germany).Antibodies used for immunoblot analysis included anti-phospho-AMPK (pAMPK; #2535) from Cell Signaling Technology (Leiden, The Netherlands), hFAB Rhodamine anti-β-actin (#12004164), and IgG StarBright Blue 700 secondary antibody (#12004162) from Bio-Rad. Tetramethylrhodamine ethyl ester (TMRE; #11560796) was obtained from Invitrogen, and MitoView™ Green (MVG; #70054) from Biotium, Inc. (Fremont, CA, USA). Icariin (molecular weight 676.66 g/mol; purity ≥99.06%; #HY-N0014) was purchased from MedChemExpress (Sollentuna, Sweden). The combined product containing adaptogenic plant extracts, Adapt Life Energy Boost (#7392213640009), was manufactured by Swedish Herbal Institute (Gothenburg, Sweden) and purchased from a local pharmacy.

1.2. *Caenorhabditis elegans* strains

The following Caenorhabditis elegans strains were used in the present study: wild-type Bristol N2; CB1370 [*daf-2*(*e1370*) III]; MIR13 [*sir-2.1*(*ok434*) IV; *aak-2*(*ok524*) X]; RB754 [*aak-2*(*ok524*) X]; MAH240 *sqIs17* [p*hlh-30*HLH-30::GFP + *rol-6(su1006)*]; LD1 *ldIs7* [SKN-1B/C::GFP + *rol-6(su1006)*]; OH16024 *daf-16* [ot971(*daf-16*::GFP) I] и SJ4143 *zcIs17* [*ges-1*::GFP(mit)]. All strains were obtained from the Caenorhabditis Genetics Center (CGC, University of Minnesota, MN, USA).

2. Methods

2.1. Preparation of leaf extract from *Punica granatum*

The seeds of *Punica granatum* L. were generously provided by the Medicinal Plant Garden at the Medical University of Lublin, Poland. Following germination and a growth period, the leaf biomass was harvested. The plant material was frozen, ground, and lyophilized using a VirTis BenchTop Pro with Omnitronics™ (Genevac Ltd, Ipswich, UK). Extraction was performed using 50% methanol (plant material to solvent ratio 1:30, w/v) in an ultrasonic bath for 20 minutes at room temperature. The obtained extract was filtered and concentrated using a rotary vacuum evaporator at 40 °C, and subsequently stored at −20 °C until further use.

2.2. Preparation of juice from *Punica granatum* fruits

Whole pomegranate fruits were purchased from a local grocery store, allowed to acclimate to room temperature, and sorted for uniformity, with fruits exhibiting physical defects being excluded. Pomegranate juice was obtained by mechanically pressing halved fruits using a juicer. The resulting juice was lyophilized using a VirTis BenchTop Pro with Omnitronics™ (Genevac Ltd, Ipswich, UK) and stored at −20 °C until further use.

2.3. Nuclear magnetic resonance (NMR) spectroscopy

Sample preparation, spectral acquisition, and data processing were performed according to a previously described methodology (Savova et al., 2021). Proton (^{1}H) and two-dimensional NMR spectra were recorded on a Bruker AVII+ 600 spectrometer (Karlsruhe, Germany). The acquired data were processed using the specialized software MestReNova (version 12.0.0, Mestrelab Research, Santiago de Compostela, Spain). Compound identification in the pomegranate leaf extract was carried out by comparing the obtained spectral data with those reported in the literature.

2.4. *C. elegans* and experimental treatment

Nematodes were cultured on NGM agar plates using *E. coli* OP50 as a food source. Age-synchronized populations were obtained by standard bleaching of reproductively active adults using a NaOH (5 N) and sodium hypochlorite (5%) solution (1:2). Following hatching, larvae were maintained under standard conditions during the L1 and L2 stages. During treatment (L3, L4, and adulthood), nematodes were fed heat-inactivated (65 °C, 30 min) and 10× concentrated *E. coli* OP50 to prevent bacterial metabolism from altering the tested compounds.

Icariin (10, 50, and 100 μM), *P. granatum* leaf extract (50, 100, and 200 μg/mL), juice (50, 100, and 200 μg/mL), and ADAPT-232 (50, 100, and 200 μg/mL) were administered at concentrations selected based on literature data and/or viability assays. A vehicle control (0.2% DMSO) was included for comparison.

For experiments targeting impaired lipid metabolism and mitochondrial dysfunction, glucose was added to the culture medium at a final concentration of 2%.

2.5. Phenotypic assessment – locomotor activity

Upon reaching the young adult stage, nematodes from all experimental groups were treated with the respective concentrations of the tested extracts or compounds for 5 and 10 days. Locomotor activity was assessed on days 5 and 10 by measuring body bends. Fifteen nematodes per group were randomly selected, transferred into a drop of M9 buffer, and allowed to acclimate for 30 s. The number of body bends was then recorded over a 30 s interval using a stereomicroscope (Kern and Sohn GmbH, Balingen, Germany). The assay was performed in three independent biological replicates.

2.6. Phenotypic assessment – reproductive capacity

For the assessment of reproductive capacity, at least five nematodes per experimental group were randomly selected and treated with the tested extracts or pure compounds. Upon reaching sexual maturity, the number of eggs laid by each individual was recorded daily throughout the reproductive period. All experiments were performed in three independent biological replicates.

2.7. Morphological parameters

Morphological parameters of *C. elegans*, including mean body length, width, and area, were analyzed using the automated nematode tracking system WormLab (MBF Bioscience).
Videos of 1 min duration were recorded and subsequently analyzed using WormLab software (version 3.1.0, MBF Bioscience; Yue et al., 2021; Sun et al., 2016). Experiments were conducted in three independent biological replicates, each including at least 15 nematodes.

2.8. Viability assesment

The absence of toxicity or adverse effects on viability following treatment with icariin (0.1–100 μM) and *P. granatum* leaf extract and juice (10–200 μg/mL) was evaluated using an MTT

assay (Yellurkar et al., 2021). Briefly, L1-stage nematodes were exposed to the treatments for 48 h, washed with M9 buffer, and incubated with MTT solution (5 mg/mL) for 3 h. Following formazan crystal formation, the reagent was removed and samples were incubated with DMSO for 1 h to ensure complete solubilization. Absorbance was measured at 575 nm using an Anthos Zenyth 340 spectrophotometer (Biochrome, Berlin, Germany).

2.9. Lifespan analysis

For lifespan assessment, at least 30 individuals from a synchronized population at the late L4 stage were randomly selected and transferred to fresh medium containing the respective treatments. This time point was designated as day 0. Nematodes were monitored daily, and survival was determined by applying a gentle mechanical stimulus using a platinum wire. Individuals that failed to respond were scored as dead. The experiment was continued until the death of the last individual in each group and was performed in three independent biological replicates.

2.10. Chemotaxis analysis

The NGM agar plates were divided into four quadrants. Two opposite quadrants containing the respective treatments were designated as test zones, while the remaining two quadrants containing inactivated E. coli OP50 served as controls. In each quadrant, 2 μL of the corresponding sample was pipetted at an equal distance from the center and allowed to dry. Approximately 100–150 L4-stage nematodes in 2 μL of M9 buffer were placed at the center of the plate. After incubation for 1 h at 20 °C, plates were transferred to 4–6 °C for 30 min to immobilize the nematodes for counting. The total number of worms and their distribution across quadrants were recorded. The chemotaxis index (CI) was calculated as:

CI = [(number of worms in test quadrants) − (number of worms in control quadrants)] / total number of worms.

2.11. Stress models – heat and oxidatives stress

To model stress conditions, nematodes were exposed to thermal and oxidative stress at two time points – day 5 and day 10 of adulthood, representing young and aged individuals. At least 30 nematodes per group were used, and survival was assessed microscopically using a gentle mechanical stimulus. All experiments were performed in three independent biological replicates.

For thermal stress, icariin-treated nematodes were exposed to 37 °C, and survival was monitored every 2 h for up to 14 h. In the experiments involving *P. granatum* leaf extract, juice, and ADAPT-232, thermal stress was induced at 37 °C for 2 h, followed by a 20 h recovery period at 20 °C.

Oxidative stress was induced by supplementing NGM medium with methyl viologen (50 mM). Pre-treated nematodes were exposed to oxidative conditions, and survival was recorded every 24 h using the same scoring criteria.

2.12. Nile Red lipid staining

Lipid accumulation in *C. elegans* was assessed using the lipophilic dye Nile Red. Following 24 h treatment, approximately 1000–1500 L4-stage larvae were collected, washed three times with M9 buffer, and fixed in 40% isopropanol for 3 min. After centrifugation, samples were incubated with Nile Red working solution in the dark for 2 h. The dye was then removed, and the pellet was washed with PBS containing 0.01% Triton X-100 (PBST) for 30 min, followed by resuspension in 100 μL PBST. For microscopy, 7 μL of each sample was mounted on glass slides. Lipid accumulation was visualized using a Stellaris 5 confocal system with a DMi8 microscope (Leica, Wetzlar, Germany). Fluorescence intensity was quantified using ImageJ (version 1.54) according to a previously described protocol (Savova et al., 2021). All experiments were performed in three independent biological replicates.

2.13. Colorimetric quantification of triglycerides

Triglyceride content in nematodes cultured in glucose-supplemented medium was measured using a commercial triglyceride assay kit (MAK266, Sigma-Aldrich). Approximately 500 nematodes per group were collected in three biological replicates. Sample preparation, measurements, and calculations were performed according to the manufacturer's instructions. Triglyceride levels (nM) were normalized to the vehicle-treated group (+G) and expressed in arbitrary units.

2.14. Assessment of mitochondrial dynamics

Mitochondrial function was evaluated by measuring mitochondrial membrane potential ($\Delta\Psi m$) using TMRE and mitochondrial mass using MVG. The dual-staining methodology was based on adapted protocols described by Berry et al. (2023) and Daskalaki et al. (2023), with minor modifications. Stock solutions of TMRE and MVG were prepared in DMSO at concentrations

of 100 μM and 200 μM, respectively. Working solutions were prepared by dilution in heat-inactivated, concentrated E. coli OP50 culture containing the respective concentrations of the tested plant extract or compounds. Final dye concentrations were 100 nM for TMRE and 4 μM for MVG. For each experimental group, at least 1000 synchronized L4-stage nematodes were used in three biological replicates and incubated with the dyes for 24 h. Following staining, nematodes were thoroughly washed with M9 buffer and allowed to recover for 1 h on bacteria-containing medium without dyes to eliminate residual fluorescence from the intestinal tract.

Imaging was performed using a Stellaris 5 confocal microscope system equipped with an inverted DMi8 microscope (Leica Microsystems). Quantitative analysis of fluorescence intensity was carried out using ImageJ software (version 1.54), according to the protocol described by Berry et al. (2023).

2.15. Expression and cellular localization in transgenic strains

To visualize the expression and cellular localization of the transcription factors HLH-30, DAF-16 и SKN-1 the transgenic lines MAH240 *sqIs17* [p$_{hlh-30}$HLH-30::GFP + *rol-6(su1006)*], OH16024 *daf-16* [ot971(*daf-16*::GFP) I] и LD1 *ldIs7* [SKN-1B/C::GFP + *rol-6(su1006)*] were used. Each experimental group consisted of a synchronized population of more than 1000 L4-stage nematodes, pre-treated for 24 h. Nematodes were then washed with M9 buffer, anesthetized with levamisole (5 mM), and mounted on glass slides. GFP fluorescence was visualized using a Stellaris 5 confocal microscope equipped with an inverted DMi8 microscope (Leica Microsystems) at 10× or 20× magnification.

Where required, a positive control was included by subjecting nematodes to acute heat stress (37 °C for 5 min) immediately prior to imaging to induce nuclear translocation of the respective transcription factors. All experiments were performed in three independent biological replicates.

2.16. Confocal microscopy and data analysis

Confocal fluorescence images of nematodes from each experimental group were acquired using a Stellaris 5 confocal microscope with an inverted DMi8 microscope (Leica Microsystems). Images were analyzed using ImageJ software (version 1.53t), and fluorescence intensity was quantified as corrected total cell fluorescence (CTCF). The obtained values were normalized to the control group and expressed in arbitrary units (a.u.).

2.17. Quantitative real-time PCR (RT-qPCR) analysis of mRNA

Total RNA was isolated using the phenol-based reagent PureZol (#7326809, Bio-Rad) from approximately 3000–4000 nematodes per group in three independent biological replicates. RNA purity, integrity, and concentration were assessed by agarose gel electrophoresis and UV spectrophotometry. Reverse transcription was performed using a First Strand cDNA Synthesis Kit (Canvax, Córdoba, Spain). mRNA expression levels were quantified using the ΔΔCt method with CFX Maestro software (Bio-Rad). The genes *iscu-1* and *mdh-1* were used as reference genes. Results were normalized to the control group.

2.18. Immunoblot analysis of protein expression

Total protein lysates from approximately 2500 nematodes per experimental group were prepared and analyzed by Western blot, as previously described (Vasileva et al., 2021). Protein extraction was performed using RIPA lysis buffer, and total protein concentration was determined using the Bradford assay. Equal amounts of protein were separated by SDS–PAGE and transferred onto nitrocellulose membranes using a Trans-Blot Turbo semi-dry transfer system (Bio-Rad). Membranes were blocked for 1 h at room temperature in 5% non-fat milk in Tris-buffered saline (TBS), followed by overnight incubation with the appropriate primary antibodies.

Detection was performed using species-specific secondary antibodies conjugated to StarBright Blue 700, and fluorescence intensity was measured using a ChemiDoc MP imaging system (Bio-Rad). Protein expression levels were normalized to the reference protein β-actin using Image Lab software (version 6.0.1, Bio-Rad).

2.19. Statistical analysis

Statistical analyses were performed using SigmaPlot v11.0 (Systat Software GmbH, Erkrath, Germany). Data are presented as mean ± standard error of the mean (SEM), where n denotes the number of independent observations used for the calculation. Depending on the analysis, n may correspond to the total number of nematodes across three independent biological replicates. Differences between experimental groups were evaluated using one-way analysis of variance (ANOVA) followed by Tukey's post hoc test. For non-normally distributed data, ANOVA on ranks followed by Dunn's test was applied, while comparisons between two groups were performed using the Mann–Whitney rank sum test. A value of $p < 0.05$ was considered statistically significant. Survival analyses for oxidative stress resistance and

lifespan assays were conducted using Kaplan–Meier survival curves. Differences between groups were assessed using the log-rank test, with statistical significance set at $p < 0.05$.

V. RESULTS

Through an ethnopharmacological selection approach, plant-derived natural products with the potential to modulate evolutionarily conserved ageing mechanisms were identified. The investigated materials included a biologically active substance (icariin), plant extracts (from Punica granatum leaf biomass and the standardized product ADAPT-232), and a functional food (juice from P. granatum fruits).

1. Evaluation of the effects of icariin on stress resistance and lifespan in *Caenorhabditis elegans*

Icariin is a naturally occurring flavonoid predominantly found in plants of the genus Epimedium. Numerous studies have extensively documented its ability to modulate inflammatory signaling pathways and cytokine production (El-Shitany et al., 2019; Zhang et al., 2017). In addition, icariin has been shown to exert atheroprotective and neuroprotective effects (Li L. et al., 2022; Wang et al., 2020). In contrast to these well-established properties, its potential role in ageing and longevity remains relatively underexplored.

1.1. Physiological parameters assessment and lifespan evaluation

To evaluate the safety of icariin in *C. elegans*, a viability assay was performed (Yellurkar et al., 2021). During the larval stages (L1–L4), nematodes were exposed to varying concentrations of icariin (10–200 μM; Fig. 12A) for 48 h. The results demonstrated no detectable toxic effects in either the wild-type (N2) or the mutant strain daf-2. Based on these findings, concentrations of 10, 50, and 100 μM were selected for subsequent analyses.

To further evaluate the potential effects of icariin on nematode physiology, additional phenotypic assays were performed. Chemotaxis analysis was conducted to assess the response to external stimuli, providing insight into the functionality of the neurosensory network involved in processes such as food-seeking behavior and avoidance of toxic substances (Queirós et al., 2021). In *Caenorhabditis elegans*, chemotactic behavior is regulated by neuroendocrine mechanisms, including *daf-7*, a homolog of human TGF-β implicated in dauer larva formation (De-Souza et al., 2023).

The chemotaxis assay revealed no significant differences between control and icariin-treated groups in either the N2 strain or the *daf-2* mutant (Fig. 12B). These findings suggest that icariin does not affect neurosensory function and further support its safety profile within the tested conditions.

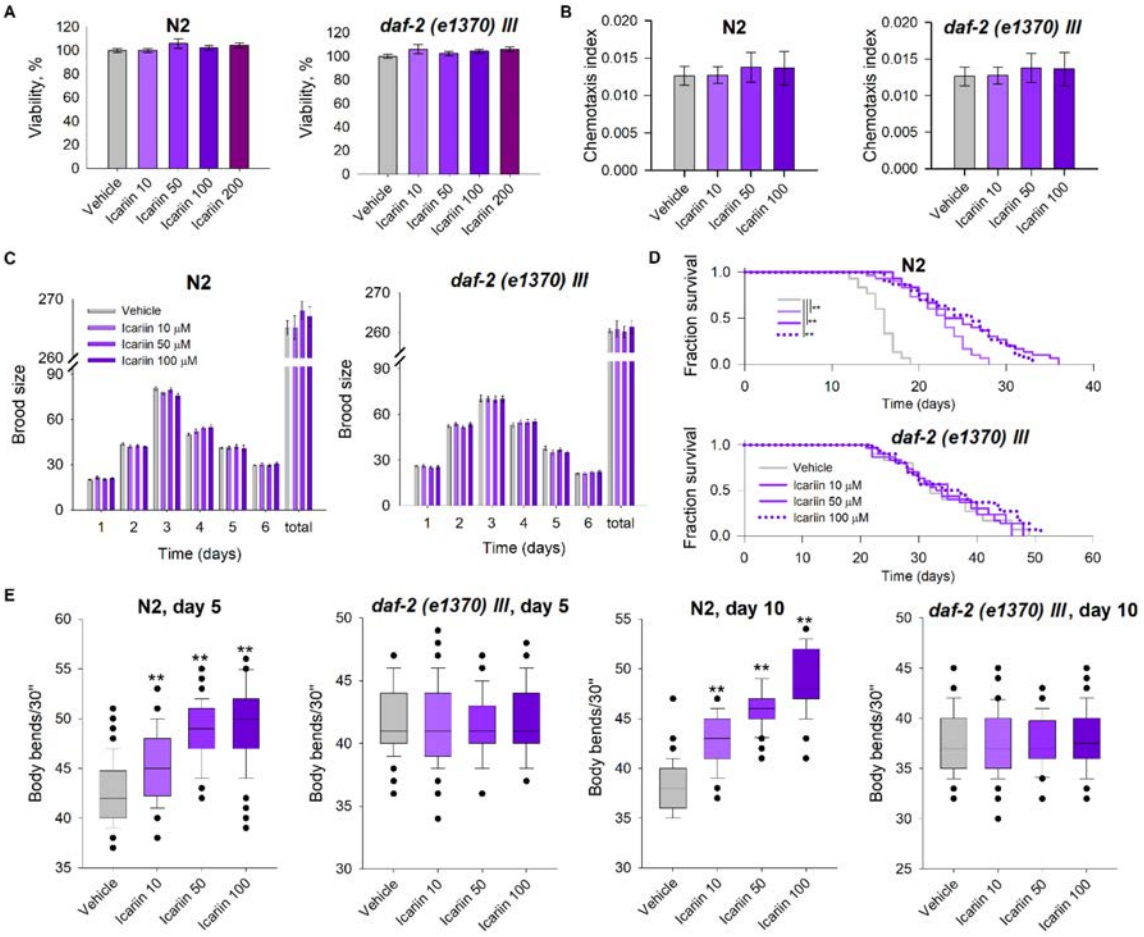

Figure 2. Icariin treatment extends lifespan, improves locomotor activity, and preserves physiological function in wild-type *Caenorhabditis elegans*, but not in the *daf-2* mutant. (A) Viability analysis of wild-type *C. elegans* (N2 strain) and *daf-2(e1370) III* mutant following icariin treatment at concentrations of 10–200 μM. (B) Chemotaxis assay in both strains after icariin treatment (n = 300–600). (C) Reproductive capacity presented as daily and total progeny in icariin-treated N2 and *daf-2* worms (n = 15). (D) Kaplan–Meier survival curves of icariin-treated worms compared to the control group (n = 90). Statistical significance between survival curves was assessed using the log-rank test. (E) Locomotor activity measured as body bends per 30 s on days 5 and 10 of adulthood in both strains (n = 45). Data in panels (B–E) are presented as mean ± SEM. Statistical significance: $p < 0.01$ vs. the respective control group (ANOVA).

To assess the effect of icariin on reproductive capacity, both daily and total progeny were quantified in treated nematodes. Reproductive output is considered a key indicator of physiological status and a hallmark of ageing in *Caenorhabditis elegans* (Spanoudakis et al.,

2023). The results showed no significant changes in fertility or brood size at any of the tested icariin concentrations (Fig. 12C), indicating that this flavonoid glycoside does not impair reproductive function in either wild-type or *daf-2* mutant worms.

Icariin treatment resulted in a statistically significant extension of lifespan in wild-type worms (Fig. 12D), whereas no such effect was observed in the *daf-2* mutant. These findings suggest a potential involvement of the DAF-2/insulin/IGF-1 signaling pathway in mediating the longevity-promoting effects of icariin.

Ageing in *C. elegans* is associated with a progressive decline in muscle function and neurodegeneration, paralleling age-related loss of motor coordination in humans and neurodegenerative disorders such as Alzheimer's and Parkinson's diseases (Sohrabi et al., 2021; Son et al., 2019). To evaluate the impact of icariin on locomotor function during ageing, body bends were quantified at two time points (days 5 and 10 of adulthood).

A dose-dependent improvement in locomotor activity was observed in wild-type nematodes following icariin treatment (Fig. 12E). In contrast, no significant improvement was detected in the *daf-2* mutant, further indicating that the beneficial effects of icariin on motor function are mediated through the DAF-2 signaling pathway and are consistent with the observed lifespan extension.

Taken together, these results demonstrate that icariin enhances locomotor activity and extends lifespan in wild-type *C. elegans* via modulation of the DAF-2/DAF-16 signaling axis. Importantly, no adverse effects on viability, neurosensory function, or reproductive capacity were observed, supporting a favorable safety profile of icariin at the tested concentrations.

1.2. Modulation of stress-resistance in young and aged individuals

To evaluate thermotolerance, nematodes pre-treated with icariin were exposed to 37 °C, and survival was monitored every 2 h over a 14 h period (Fig. 13A–D). Experiments were conducted on days 5 and 10 of adulthood, representing early and advanced stages of age-related decline. In wild-type worms, icariin significantly increased thermotolerance at all tested concentrations (10, 50, and 100 μM; Fig. 13A, C). In contrast, no significant effect was observed in the *daf-2* mutant, which is characterized by intrinsically elevated stress resistance (Bao et al., 2022) (Fig. 13B, D).

Maintenance of efficient antioxidant defense mechanisms is a key determinant of delayed ageing (Guo et al., 2022; Statzer et al., 2022). In *C. elegans*, exposure to pro-oxidants such as methyl viologen (paraquat) induces increased ROS production, neuronal damage, and

premature death. In the present study, the antioxidant potential of icariin was assessed under acute oxidative stress conditions induced by methyl viologen (50 mM), with survival monitored every 24 h until the death of the last individual (Fig. 13E–H).

On day 5, icariin treatment resulted in a dose-dependent increase in resistance to paraquat in wild-type worms, with the effect persisting up to 48 h. On day 10, a statistically significant increase in survival was observed at 24 h, while at 48 h the effect remained evident only at concentrations of 50 and 100 μM (Fig. 13E, G). In *daf-2* mutants, increased survival was also observed 24 h post-exposure on both day 5 and day 10 (Fig. 13F, H), with sustained effects at 48 h only at higher concentrations. However, complete lethality was observed in all groups by 72 h, indicating that icariin does not confer protection against cumulative oxidative toxicity.

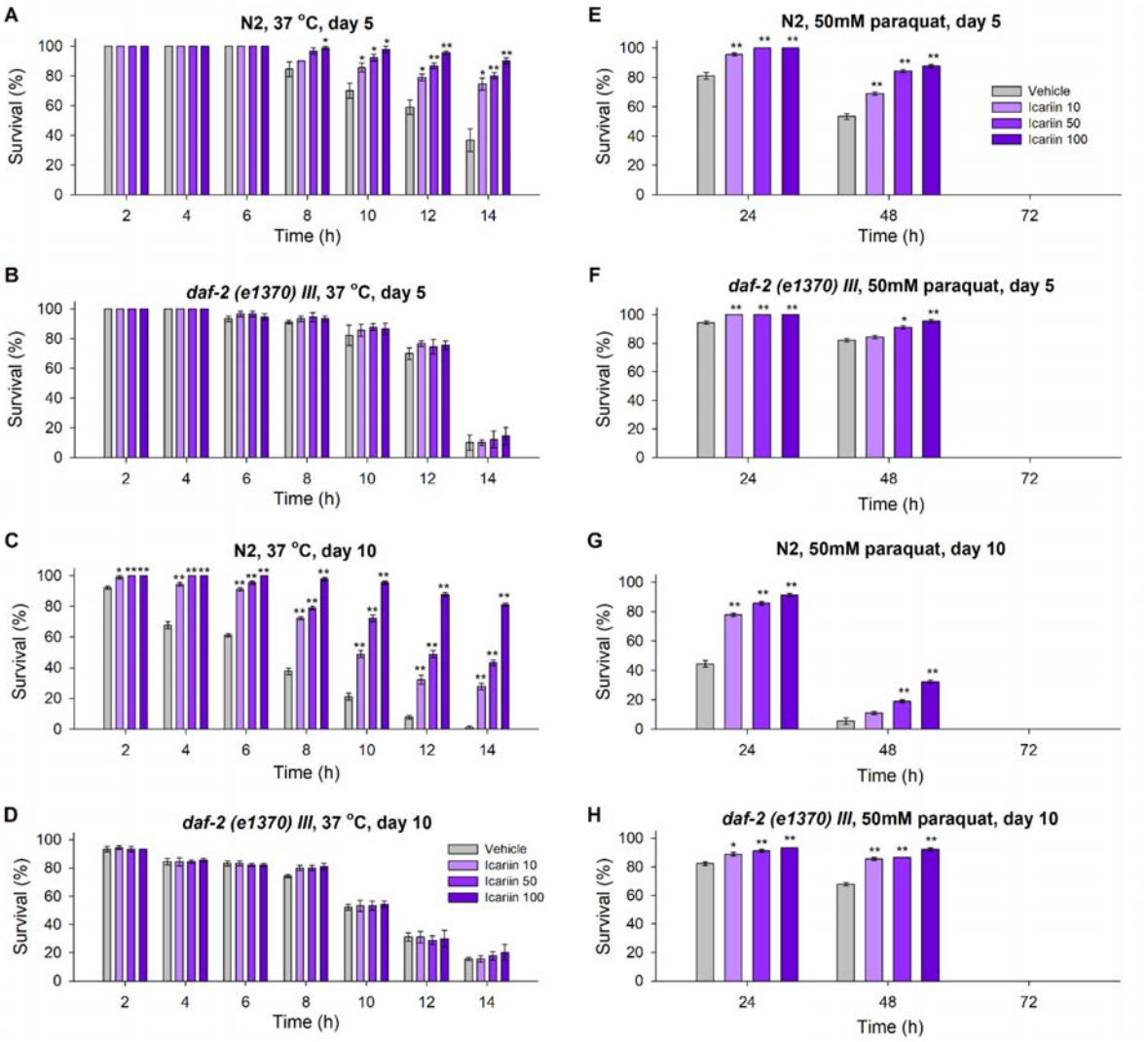

Figure 3. Icariin treatment enhances heat and oxidative stress resistance in *C. elegans*. Wild-type N2 (A,C,E,G) and daf-2 mutant (B,D,F,H) strains were subjected to treatment with

icariin at concentrations of 10, 50, and 100 μM. (A–D) For heat-stress induction, on both the 5th and 10th days of their lifespan, they were incubated at 37 °C for 14 h. The viability was monitored at two-hour intervals until the death of the last worm. (E–H) As an oxidative stressor, on day 5 and day 10 of their lifespan, the worms were exposed to a paraquat concentration of 50 mM. The resistance to oxidative stress was assessed at 24 h intervals until the death of the last worm. The results were represented as percentage survival as mean ± SEM, n = 90, * $p < 0.05$, ** $p < 0.01$ (one-way ANOVA).

In summary, icariin significantly enhances resistance to oxidative stress in both strains, suggesting that this effect is mediated through a mechanism that is independent of, or operates in parallel with, the IIS pathway. In contrast, the protective effect against thermal stress was observed only in wild-type worms, providing evidence for the involvement of IIS, given the lack of response in *daf-2* mutants. These findings indicate that icariin activates distinct protective mechanisms depending on the specific stress conditions. Overall, the data support the hypothesis that improved physiological resilience is a key component of the beneficial effects of icariin on organismal health.

1.3. Effects of icariin on basal metabolism

Several studies in *Caenorhabditis elegans* suggest a link between increased locomotor activity and elevated energy expenditure (Farias-Pereira et al., 2020; Statzer et al., 2022). In this context, the potential impact of icariin on basal lipid metabolism was investigated.

In wild-type nematodes, a statistically significant reduction in total triglyceride content was observed at concentrations of 50 and 100 μM, as determined by Nile Red staining (Fig. 14A, B).

In the *daf-2* mutant strain, which is characterized by increased lipid accumulation due to impaired insulin-like signaling (Bao et al., 2022), a lipid-lowering effect was observed only at the highest tested concentration of icariin (100 μM; Fig. 14C, D).

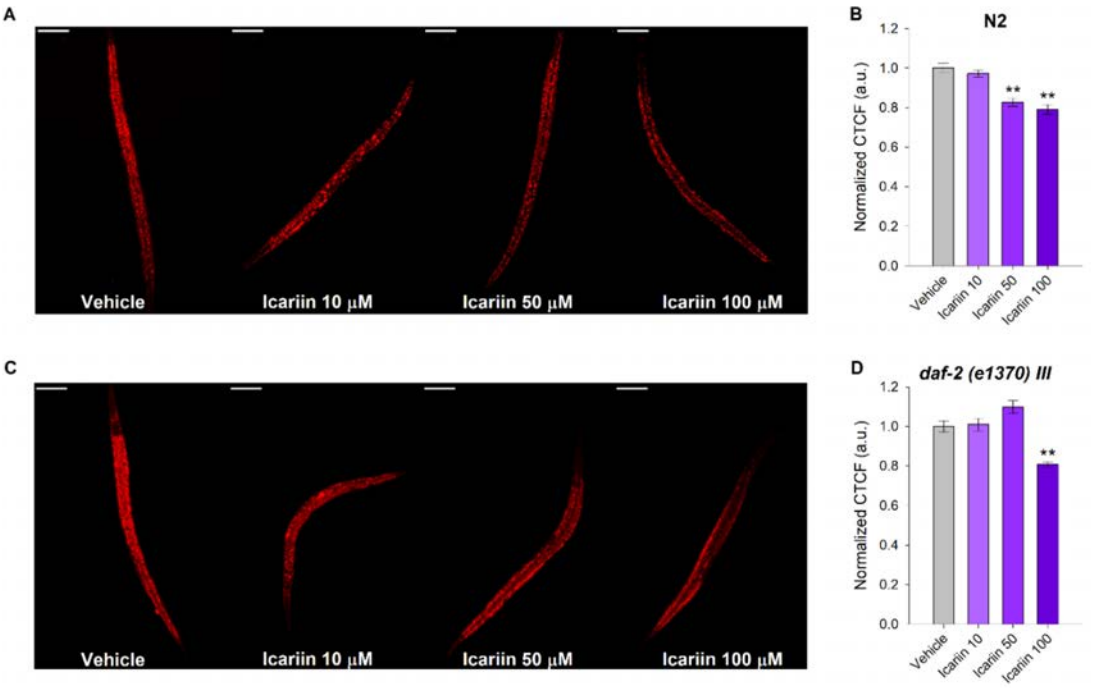

Figure 4. Icariin supplementation modulates fat metabolism in *C. elegans*. Representative confocal photographs at 20× magnification (scale bar of 50 μm) of Nile red lipid staining of wild type (a) and *daf-2* mutant strain (c) nematodes treated for 24 h with 10, 50, and 100 μM icariin or vehicle. Quantification of lipid accumulation as normalized correlated total cell fluorescence (n = 90), corrected total cell fluorescence (CTCF) expressed as arbitrary units (a.u.) as follows for wild-type (b) and *daf-2* (d) nematodes. Values are shown as mean ± SEM, ** $p < 0.01$ compared to the vehicle group (one-way ANOVA).

These results reveal a novel functional aspect of icariin as a compound with potential lipid-modulating properties, whose effects appear to be at least partially dependent on the *daf-2* pathway. At the same time, the response observed in wild-type worms at lower concentrations suggests that icariin may also act through additional molecular mechanisms independent of classical insulin-like signaling.

1.4. Gene expression analysis through RT-qPCR

To further elucidate the molecular mechanisms underlying the lifespan-extending effects of icariin, a transcriptional analysis was performed, focusing on the *daf-2*/IIS pathway as well as on key evolutionarily conserved genes involved in longevity regulation, stress resistance, and metabolic adaptation. The expression levels of *skn-1*, *sir-2.1*, *sir-2.4*, and *hsf-1* were analyzed

genes associated with cellular homeostasis and stress responses and corresponding to the human homologs NRF2, SIRT1, SIRT6, and HSF1, respectively (Jiang et al., 2021).

The obtained data provide further evidence supporting the hypothesis that icariin exerts its biological effects through inhibition of *daf-2* and modulation of the IIS pathway. Treatment with icariin at concentrations of 50 μM and 100 μM resulted in a statistically significant downregulation of *daf-2* expression (Fig. 15A), with distinct expression profiles observed between the two concentrations.

At 50 μM, suppression of *daf-2* was accompanied by increased transcriptional activity of *daf-16* (Fig. 15B) and its downstream target gene metallothionein (*mtl-1*; Fig. 15H), as well as activation of *jnk-1* (Fig. 15G), a well-established modulator of DAF-16 under cellular stress conditions (Mao et al., 2018). Concurrently, elevated expression of *skn-1* (Fig. 15E) and *hsf-1* (Fig. 15F) was observed, both of which act in parallel with *daf-16* and contribute to longevity through independent regulatory pathways (Zhang et al., 2021).

Notably, icariin treatment at 50 μM led to increased expression of *sir-2.4* (Fig. 15C), whereas no significant change was observed for *sir-2.1* (Fig. 15D), suggesting a specific involvement of this sirtuin in the mechanism of action of the compound.

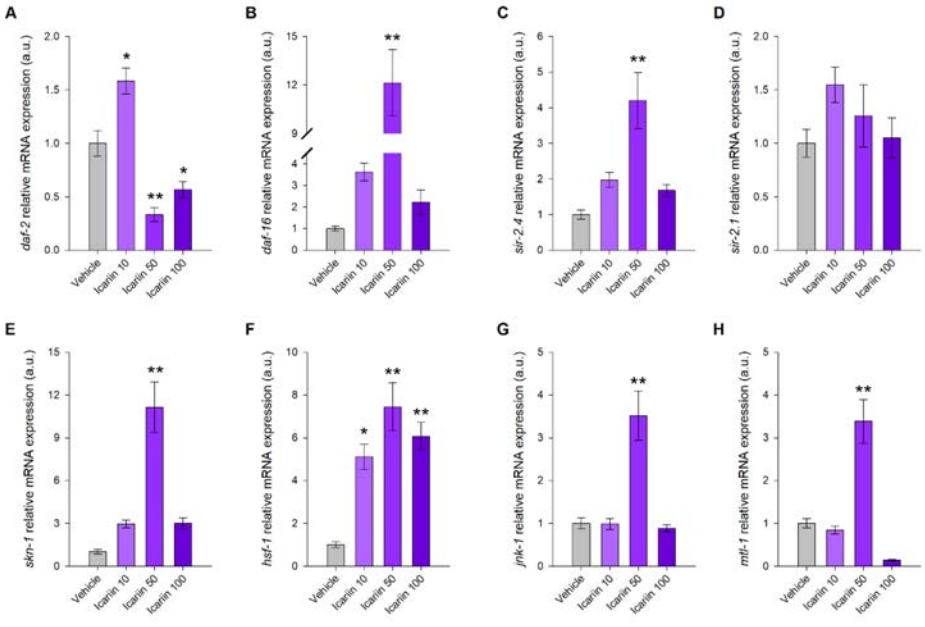

Figure 5. Icariin treatment modulates gene expression of evolutionarily conserved pro-longevity pathways in wild-type *C. elegans*. Normalized relative mRNA expression in arbitrary units (a.u.) of *daf-2* (a), *daf-16* (b), *sir-2.4* (c), *sir-2.1* (d), *skn-1* (e), *hsf-1* (f), *jnk-*

1 (g), and *mtl-1* (h) upon treatment with 10, 50, and 100 μM icariin. Data shown are mean ± SEM, n = 9. * $p < 0.05$, ** $p < 0.01$ compared to the vehicle group (one-way ANOVA).

At the higher concentration of 100 μM, a significant increase was observed exclusively in the expression of *hsf-1* (Fig. 15E), with no substantial changes detected in the levels of the other analyzed genes. This finding suggests that higher doses of icariin may induce a more targeted and restricted transcriptional response, selectively activating specific protective pathways such as those regulated by *hsf-1*. This, in turn, indicates the presence of a dose-dependent threshold at which different concentrations modulate distinct molecular networks.

Overall, the gene expression data demonstrate that *hsf-1* is the only regulator consistently activated across all tested concentrations of icariin. At 50 μM, however, a broader set of genes, including *daf-2* and *daf-16*, is modulated, indicating a more complex and coordinated protective response. In contrast, at 100 μM, the regulatory response appears to be largely confined to *hsf-1*, reflecting a more specific, dose-dependent mode of action. These findings confirm that different concentrations of icariin differentially modulate molecular mechanisms involved in longevity and cellular stress resistance.

1.5. Analysis of DAF-16 dynamics and subcellular localization

Based on the gene expression results and the central role of DAF-16 in the regulation of ageing and longevity, the effect of icariin on the subcellular localization of this transcription factor was investigated. For this purpose, the transgenic strain *daf-16(ot971[daf-16::GFP])* was used, enabling direct visualization of DAF-16 nuclear translocation.

Treatment with icariin (50 μM) resulted in increased nuclear localization of DAF-16::GFP compared to the control group, as confirmed by fluorescence microscopy imaging (Fig. 16A, B). These findings are fully consistent with the transcriptional data (Fig. 16B) and further support the conclusion that the effects of icariin at 50 μM are, at least in part, mediated through DAF-16.

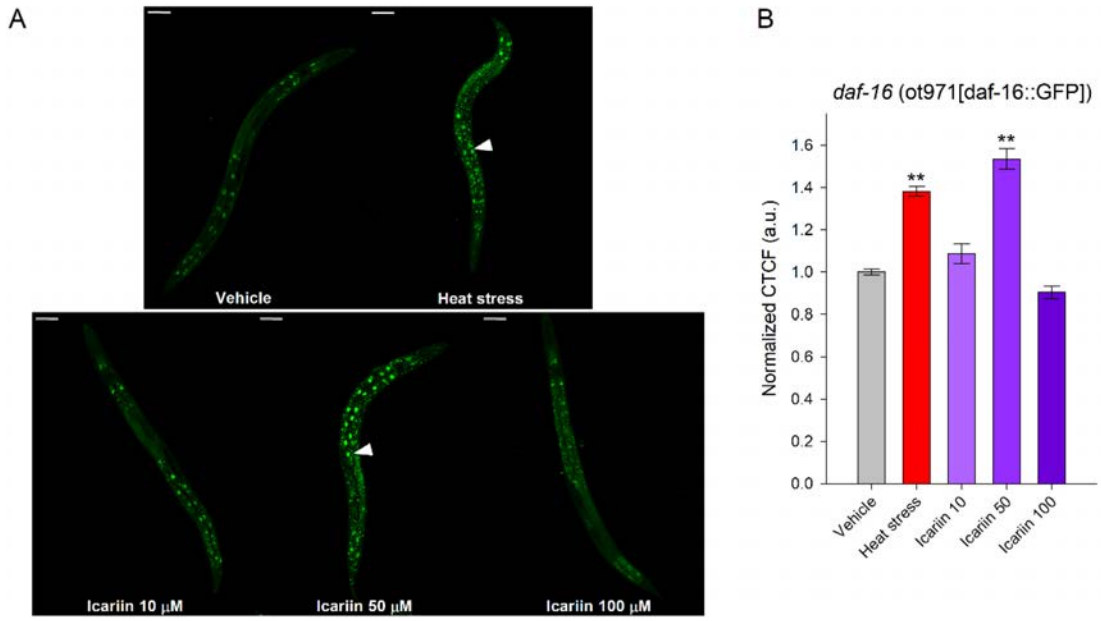

Figure 6. Nuclear translocation of DAF-16 was observed upon icariin treatment. Evaluation of nuclear translocation of *daf-16(ot971[daf-16::GFP])* mutant strain. (a) Representative fluorescent confocal microphotographs at 20× magnification (scale bar of 50 μm) of vehicle, heat-shocked control (37 °C for 5 min) or icariin-treated *C. elegans daf-16(ot971[daf-16::GFP]).* Arrowheads indicate increased nuclear localization. (b) Using ImageJ version 1.53t, the fluorescent signal was processed to cell total correlates fluorescence (CTCF), normalized to the vehicle group, and represented in arbitrary units (a.u.). The data are shown as means ± SEM, n = 60, ** $p < 0.01$, compared to the vehicle (one-way ANOVA).

2. Metabolic profiling and evaluation of the potential of *Punica granatum* leaf extract to modulate ageing processes

Листата на Pomegranate leaves represent a non-edible plant by-product characterized by a high content and diversity of secondary metabolites. Their rich phytochemical profile defines them as a valuable source of bioactive compounds. Among the most prominent constituents identified in pomegranate leaf extracts are flavonols, flavones, and tannins (Machado et al., 2022).

The *P. granatum* leaves are emerging as promising candidates for the therapeutic regulation of metabolic processes; however, their potential to modulate ageing-related pathways remains insufficiently explored (Chattopadhyay and Thirumurugan, 2018; Maphetu et al., 2022).

2.1 Metabolite profiling by NMR spectroscopy

Pomegranate leaves are non-edible byproduct with a rich phytochemical composition, which may be utilized either for their medicinal properties or as a functional ingredient. The most characteristic compounds for PGL extracts reported in the literature are flavonols, flavones, and tannins (Machado et al., 2023). Metabolite profiling of PGL extract was performed through comparison of the obtained proton and 2D ($^{1}H^{1}H$–-COSY and $^{1}H^{13}C$–-HSQC) spectra with the literature data (Savova et al., 2021; Sudjaroen et al., 2012; Wolfender et al., 2013). Some common primary and secondary metabolites (as epicatechin, methyl gallate, and corilagin) were identified upon evaluation of ^{1}H spectra. Zoom-in of the proton spectrum and assignments of the identified metabolites are represented in Fig. 1A and 1B. Corresponding chemical shifts (δ, ppm) and coupling constants (J, Hz) are listed in Supplementary Table S4. The presence of corilagin was confirmed upon further interpretation of the 2D ($^{1}H^{1}H$–-COSY and $^{1}H^{13}C$–-HSQC) spectra of PGL extract and comparison with the literature data (Sudjaroen et al., 2012). The coupling between the protons ($^{1}H^{1}H$–) in the glucose moiety of corilagin were also found in the COSY spectra (Fig. 1C) of PGL. Within the HSQC (Fig. 1D) spectra of PGL, were found cross-peaks between ^{1}H and ^{13}C which correspond to the signals from three aromatic rings as follows for carbons - C3 (δ_H 6.68-δ_C 107.88), C3′ (δ_H 6.71-δ_C 109.81), C2″ and C6″ (δ_H 7.06-δ_C 110.09). The signals from α-D-glucose moiety were assigned in HSQC spectrum for C-2‴ (δ_H 3.99-δ_C 69.59), C-4‴ (δ_H 4.6-δ_C 69.59), C-5‴ (δ_H 4.55-δ_C 75.54) and for anomeric carbon at position C1‴ (δ_H 6.48-δ_C 94.14).

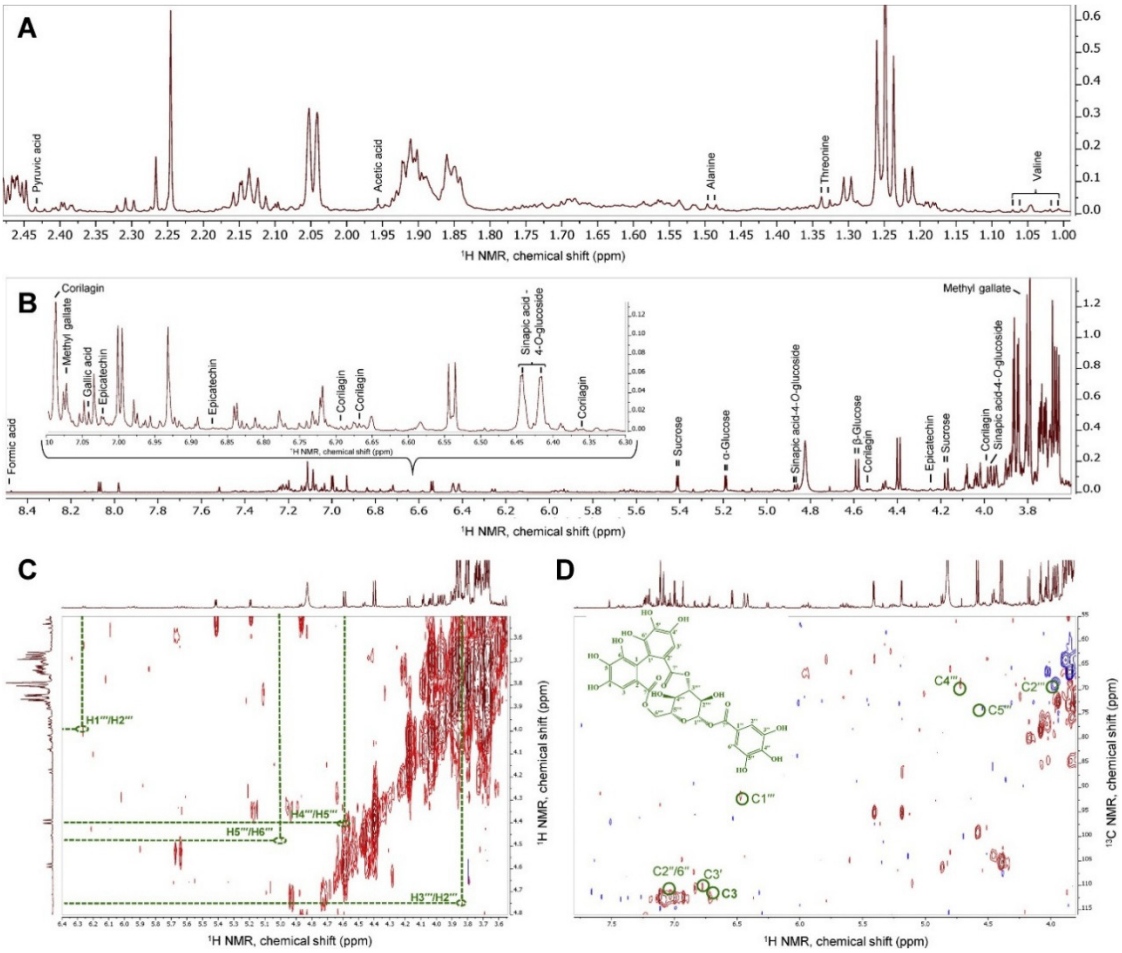

Figure 7. Representative NMR spectra of *Punica granatum* leaf extract. Assignments of identified primary and secondary metabolites in PGL extract the proton NMR spectra at (A) δ 1–2.5 ppm, and (B) δ 3.5–8.5. Zoomed-in (C) $^{1}H^{1}H$– homonuclear correlation spectrum (COSY) and (D) $^{1}H^{13}C$– heteronuclear single quantum coherence spectrum (HSQC) with annotated characteristic signals of corilagin (Molecular weight 634.5 g/M; IUPAC name [(1S,19R,21S,22R,23R)−6,7,8,11,12,13,22,23-octahydroxy-3,16-dioxo-2,17,20-trioxatetracyclo[17.3.1.04,9.010,15]tricosa-4,6,8,10,12,14-hexaen-21-yl] 3,4,5-trihydroxybenzoate).

2.2 Lifespan and phenotypic analysis

Prior to evaluating the effects of *P. granatum* leaf extract on lifespan, its safety was assessed using a viability assay in *Caenorhabditis elegans*. The extract was administered at concentrations ranging from 10 to 200 µg/mL for 48 h during the larval stages (L1–L4), with no detectable toxicity observed (Fig. 18A).

Based on these results, concentrations of 50, 100, and 200 µg/mL were selected for subsequent experiments.

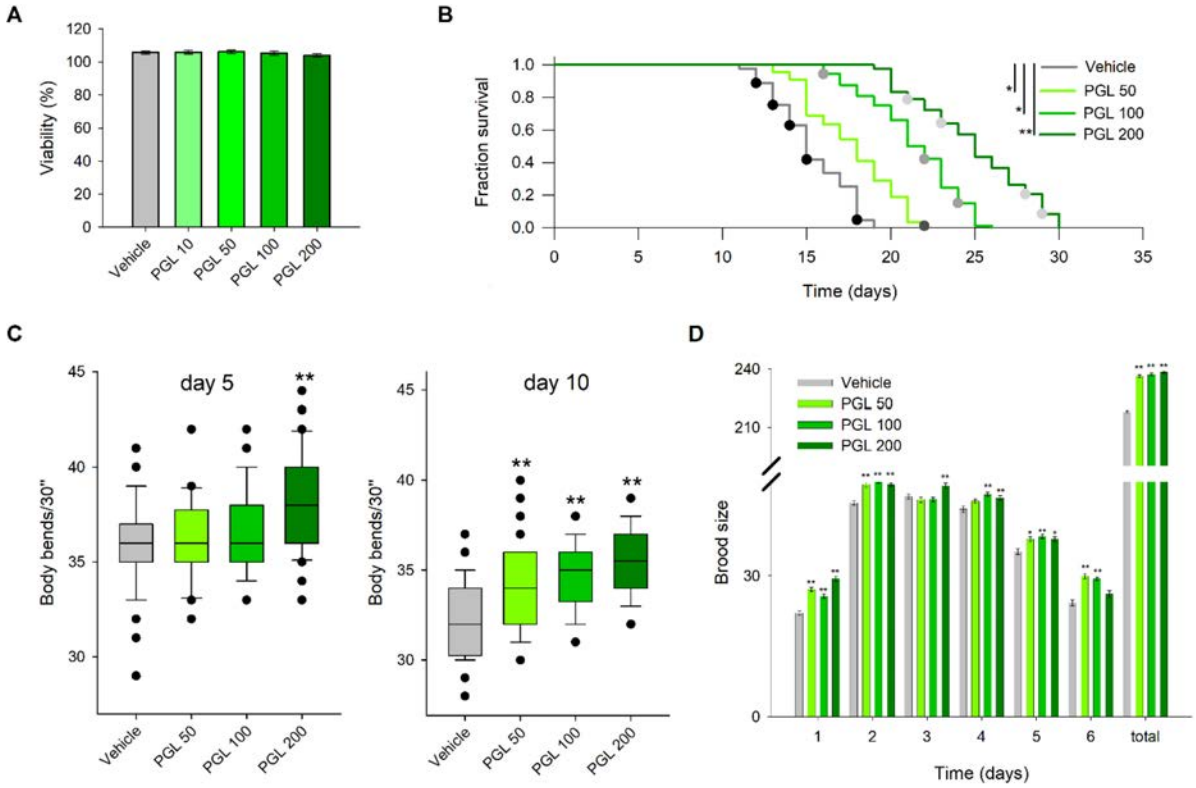

Figure 8. Pomegranate leaf extract extends lifespan, enhances mobility and increases brood size of wild-type *C. elegans*. (A) Viability test upon treatment with PGL extract (10–200 µg/ml). (B) The lifespan of nematodes exposed to PGL extract treatment (50, 100 and 200 µg/ml). (C) Numbers of body bends in 30-seconds on both day 5 and day 10 of lifespan (n = 45). (D) Total brood size of PGL-treated wild-type (N2) *C. elegans* (n = 15). Data for B, C, and E are presented as mean ± SEM, $*p < 0.05$, $**p < 0.01$ compared to vehicle group by one-way analysis of variance (ANOVA). The comparison of the lifespan between PGL extract treated worms and the vehicle group was performed using a Kaplan-Meier survival curve, represented as a fraction survival (n = 90). The statistical significance of the survival curves was assessed using the Log-rank test.

Lifespan analysis revealed that treatment with PGL (50, 100, and 200 µg/mL) resulted in a statistically significant extension of lifespan in wild-type *Caenorhabditis elegans* (N2), with a clear dose-dependent effect observed (Fig. 18B).

Locomotor activity was assessed by measuring body bends on days 5 and 10 of adulthood. PGL treatment significantly improved locomotor performance at both time points compared to the control group (Fig. 18C).

To further evaluate physiological status, reproductive capacity was assessed by quantifying daily and total progeny. PGL treatment led to a significant increase in fertility compared to controls (Fig. 18D).

Collectively, these phenotypic and lifespan data demonstrate that PGL has the potential to promote healthy ageing by delaying age-related functional decline, enhancing reproductive capacity, and preserving locomotor activity in *C. elegans*.

2.3 Lipid homeostasis and involvement of key metabolic regulators

To investigate the effects of PGL on metabolic processes, basal lipid metabolism was assessed. Treatment with PGL at concentrations of 100 and 200 μg/mL resulted in a significant reduction in lipid levels compared to the control group (Fig. 19A, B).

To explore the underlying mechanisms, transcriptional analysis was performed, revealing that PGL treatment (100 and 200 μg/mL) significantly upregulated the expression of *hlh-11* (Fig. 19D), *aak-2* (Fig. 19F), and *sir-2.1* (Fig. 19G), suggesting activation of key pathways involved in energy metabolism, particularly lipid oxidation.

To further assess the role of AMPK in the mechanism of action, immunoblot analysis was conducted to determine the levels of phosphorylated AMPK (pAMPK). No significant changes in phosphorylation levels were observed compared to the control group (Fig. 19H), indicating that the regulation of lipid metabolism is likely mediated at the transcriptional level rather than through post-translational activation of AMPK.

Notably, a statistically significant induction of *hlh-30* expression was observed at all tested PGL concentrations (Fig. 19E). As a homolog of human TFEB, *hlh-30* is a key transcription factor regulating lysosomal biogenesis, autophagy, and metabolic adaptation. In parallel, downregulation of *let-363* expression (Fig. 19C), corresponding to inhibition of mTOR signaling, was observed, which is consistent with the effects on metabolism and cellular resilience.

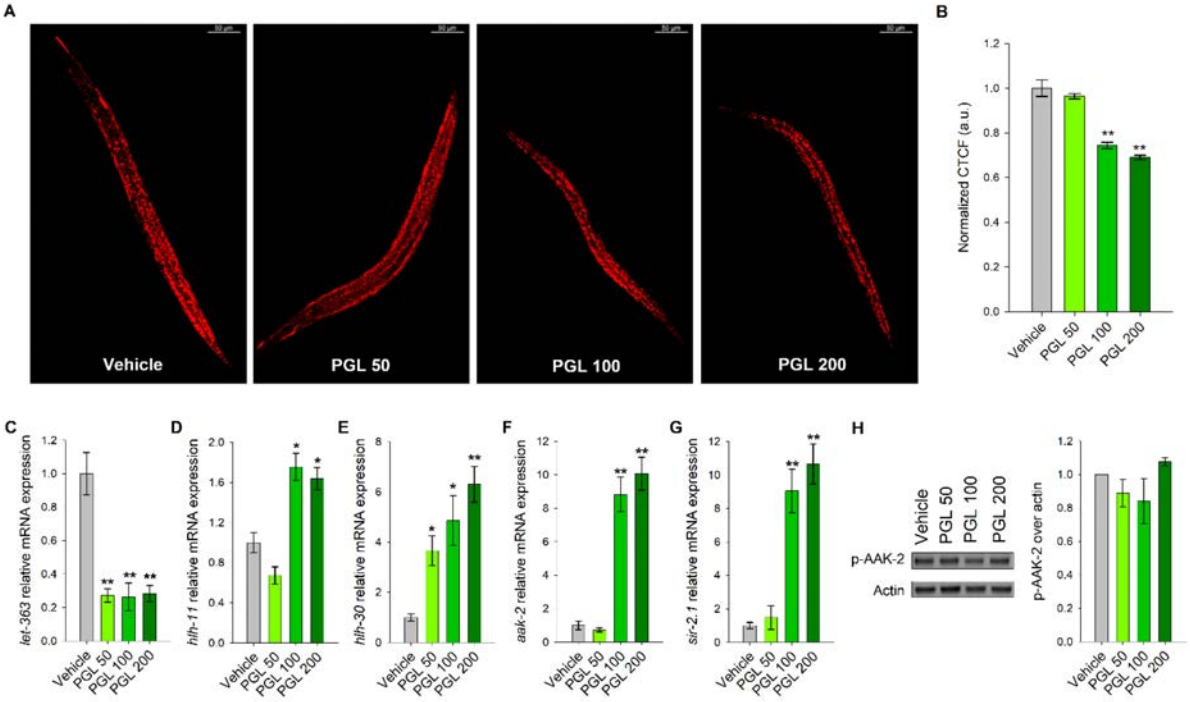

Figure 9. Regulation of lipid accumulation and metabolism homeostasis by PGL supplementation. (A) Representative confocal photographs at 20x magnification (scale bar of 50 μm) of Nile red staining of lipid deposition in wild-type N2 worms with vehicle or PGL extract (50, 100, and 200 μg/ml) respectively. (B) Quantification of lipid accumulation as normalized to vehicle group corrected total cell fluorescence (CTCF), represented as arbitrary units (a.u.). Values are shown as mean ± SEM (n = 90), $^{*}p < 0.05$, $^{**}p < 0.01$ compared to the vehicle (one-way ANOVA). Normalized relative mRNA expression levels in arbitrary units of genes associated with metabolism regulation (C) *let-363*, (D) *hlh-11*, (E) *hlh-30*, (F) *aak-2*, and (G) *sir-2.1* following treatment with either vehicle or PGL extract. Data are expressed as mean ± SEM, n = 9, $^{*}p < 0.05$ and $^{**}p < 0.01$ compared to the vehicle (one-way ANOVA). (H) Representative image of western blot analysis of phosphorylation levels of AAK-2 (pAMPK) and its normalized expression against actin as a housekeeping protein, ± SEM (n = 3).

2.4 Effects of PGL on stress response and associated signaling pathways

To evaluate the potential of PGL to modulate stress resistance, survival was assessed in young (day 5) and aged (day 10) nematodes subjected to acute thermal or oxidative stress.

The results demonstrated that PGL treatment led to a concentration-dependent increase in survival of wild-type nematodes following a 20 h recovery period after thermal stress (37 °C for 2 h), both on day 5 (Fig. 20A) and day 10 (Fig. 20D). A similar effect was observed under acute oxidative stress induced by supplementation of the growth medium with 50 mM

methyl viologen, with increased survival on both day 5 (Fig. 20B) and day 10 (Fig. 20E) compared to the vehicle-treated group.

To further elucidate the molecular mechanisms underlying the enhanced stress resistance, transcriptional analysis was performed on a panel of genes representing key regulators of stress response and longevity, including *daf-16*, *daf-2*, *sir-2.4*, *hif-1*, flavin-containing monooxygenase 2 (*fmo-2*), *hsf-1*, and the dual-specificity mitogen-activated protein kinase kinase *sek-1* (Fig. 20G).

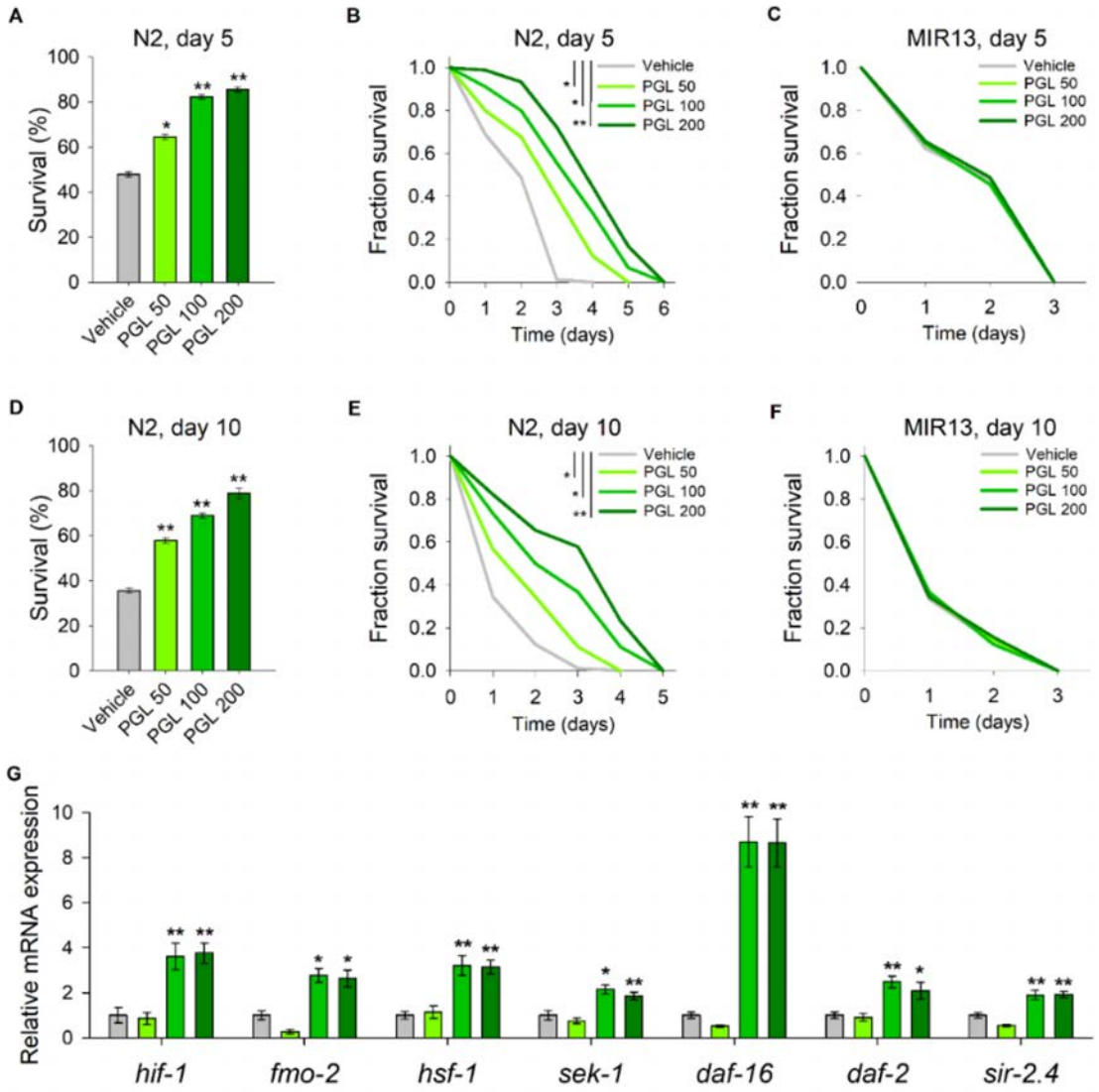

Figure 10. Supplementation with PGL extract mediates acute stress endurance through activation of multiple stress-response pathways. *C. elegans* N2 (A,B,D,E) and MIR13 [*sir-2.1*(*ok434*) IV; *aak-2*(*ok524*) X] (C,F) worms were subjected to treatment with PGL extract with concentrations of 50, 100 and 200 μg/ml or vehicle. (A,D) Survival upon of acute heat-stress exposure (37 °C for 2 h) followed by a 20-hour recovery period under normal conditions

of N2 worms (day 5 and day 10 of lifespan). The results are represented as percentage survival as mean ± SEM, $n = 90$, $^{*}p < 0.05$, $^{**}p < 0.01$ (one-way ANOVA). Survival curves following paraquat-induced oxidative stress (50 mM) in N2 (B,E) and MIR13 (C,F) worms, measured at 24-hour intervals. Sample size: $n > 90$ were scored for each treatment. Data were proceeded using Kaplan-Meier analysis, and p values were calculated using the log-rank test. (G) Normalized relative mRNA expression levels of *hif-1*, *fmo-2*, *hsf-1*, *sek-1*, *daf-16*, *daf-2*, and *sir-2.4* following treatment with either vehicle or PGL extract. Data are expressed as mean ± SEM, $n = 9$, $^{*}p < 0.05$ and $^{**}p < 0.01$ compared to the vehicle group (one-way ANOVA).

Treatment with PGL at concentrations of 100 and 200 μg/mL resulted in a statistically significant upregulation of *hsf-1* (Fig. 20G), a central mediator of the heat stress response, as well as *fmo-2* (Fig. 20G), whose activation has been associated with lifespan extension under dietary restriction conditions (Choi et al., 2023; Tuckowski et al., 2025). Increased expression of *daf-16*, *sir-2.4*, and *daf-2* (Fig. 20G) was also observed, further supporting the involvement of the insulin/IGF-1 signaling pathway in the mechanism of action. Additionally, elevated transcriptional activity of *sek-1* (Fig. 20G), the ortholog of MKK3/6 and a component of the p38 MAPK cascade, suggests activation of pathways related to innate immunity (Huang et al., 2023).

Given the observed reduction in lipid accumulation, the possibility that enhanced stress resistance is mediated through metabolic regulation was further investigated. For this purpose, the double mutant strain MIR13, lacking functional *aak-2*/AMPK and *sir-2.1*/SIRT1, was employed. Under this genetic background, no increase in oxidative stress resistance was observed following PGL treatment, either on day 5 or day 10 of adulthood (Fig. 20C, F). These findings indicate that the protective effect of PGL against oxidative stress is dependent on the activity of AAK-2 and SIR-2.1.

Overall, the results demonstrate that PGL promotes healthy ageing in *Caenorhabditis elegans* by enhancing resistance to both thermal and oxidative stress. This effect is accompanied by the regulation of key genes involved in stress response and longevity, including *daf-16*, *hsf-1*, *sir-2.4*, *sek-1*, *fmo-2*, and *hif-1*, as well as activation of metabolic sensor pathways such as *aak-2* and *sir-2.1*.

2.5 Role of HLH-30/TFEB и DAF-16/FOXO in the mechanism of action

The transcription factor HLH-30, the ortholog of human TFEB, is a key regulator of autophagy, lysosomal biogenesis, and metabolic adaptation, with its increased activity being associated with lifespan extension and improved cellular homeostasis (Lin et al., 2018; Possik et al., 2023).

In the present study, PGL treatment was found to activate HLH-30, as evidenced by increased fluorescence in the transgenic HLH-30::GFP strain (Fig. 21C, D). This observation is consistent with the upregulation of *hlh-30* expression at the transcriptional level (Fig. 19E) and supports the hypothesis that HLH-30 acts as a key mediator of the effects of PGL on healthy ageing.

The transcription factor DAF-16 plays a central role in the regulation of longevity, stress resistance, and metabolic homeostasis (Ham et al., 2024; Sen et al., 2020). Treatment with PGL at concentrations of 100 and 200 μg/mL resulted in a statistically significant increase in *daf-16* expression (Fig. 20G). To functionally validate this effect, a fluorescent reporter strain expressing DAF-16::GFP was used. Fluorescence imaging revealed enhanced nuclear translocation of DAF-16 in treated nematodes compared to controls (Fig. 21A, B), confirming its activation and involvement in the protective effects of PGL on healthspan.

Taken together, these findings support the hypothesis that PGL modulates evolutionarily conserved signaling pathways involved in both autophagy and adaptive stress responses. The activation of transcription factors such as HLH-30/TFEB and DAF-16/FOXO defines a molecular framework through which PGL exerts its potential as a natural regulator of healthy ageing and longevity.

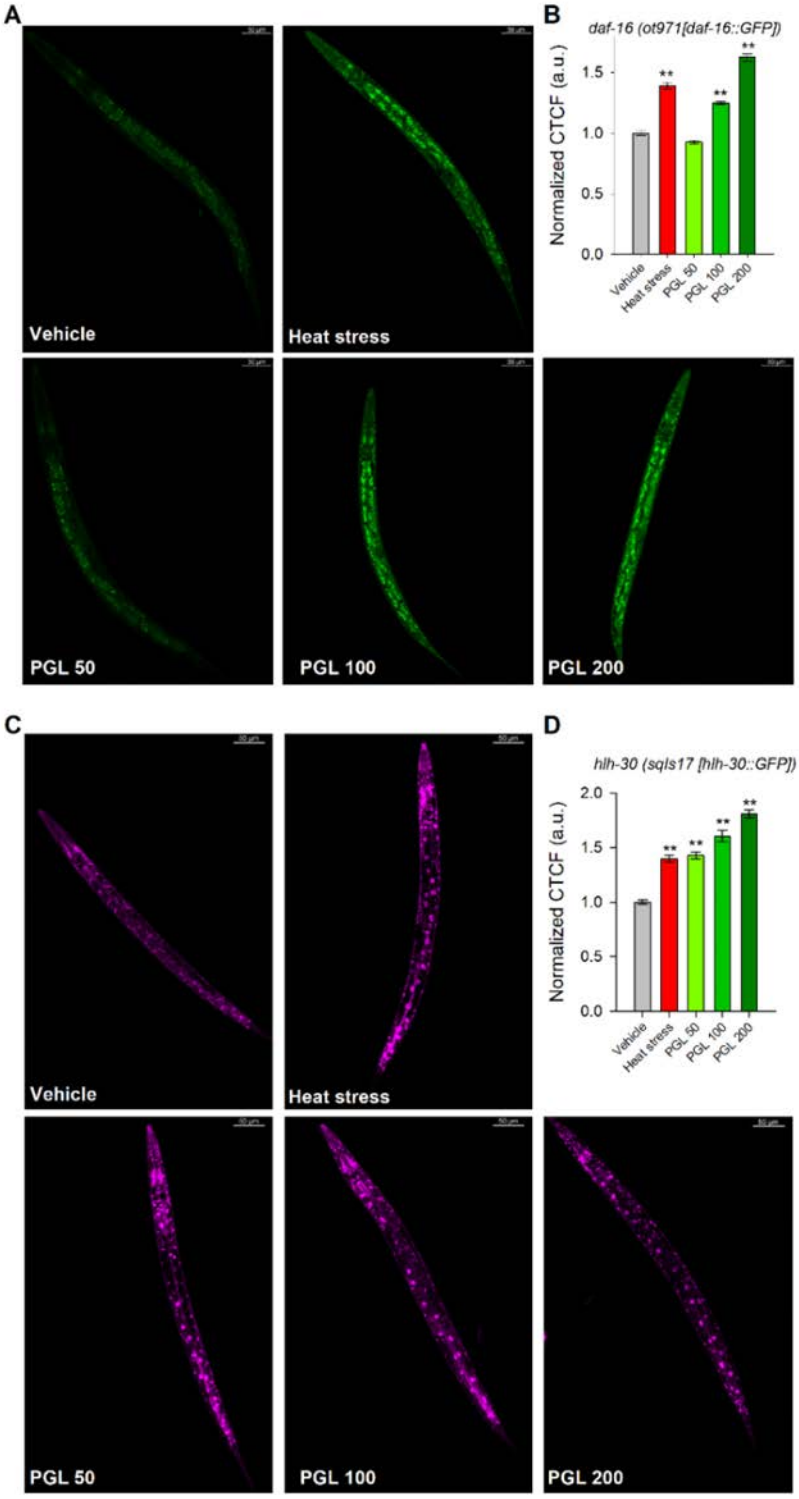

Figure 11. Effect of PGL extract on HLH-30::GFP and DAF-16::GFP transgenic strains. (A,C) Representative fluorescent confocal microphotographs at 20x magnification (scale bar of 50 μm) of vehicle, heat-stressed control (37 °C for 5 min) or PGL-treated *C. elegans* OH16024 *daf-16* [*ot971*(*daf-16*::*GFP*) I] and MAH240 *sqIs17* [*hlh-30p*::*hlh-30::GFP* + *rol-6*(*su1006*)]. (B,D) Cell total correlates fluorescence (CTCF), normalized to the

vehicle group and represented in arbitrary units (a.u.). The data are shown as means ± SEM, n = 60, $^{**}p < 0.01$, compared to the vehicle (one-way ANOVA).

2.6 Role of SKN-1/NRF2 in the mechanism of action of PGL

The transcription factor NRF2 and its *Caenorhabditis elegans* ortholog SKN-1 are key mediators of redox homeostasis and play a central role in the adaptive cellular response to oxidative stress (Banse et al., 2024; Thomas et al., 2023). To determine whether SKN-1 is involved in the mechanism of action of the pomegranate leaf extract, its activity was evaluated using the GFP-labeled transgenic strain LD1 (*skn-1::GFP*). A significant increase in nuclear localization of SKN-1::GFP was observed (Fig. 22A, B), indicating activation of SKN-1-dependent signaling.

To further validate these findings, transcriptional analysis was performed, revealing a statistically significant upregulation of *skn-1* expression (Fig. 22C), as well as its well-characterized target gene *gst-4*, a marker of SKN-1-mediated cellular response (Fig. 22D).

Taken together, the gene expression data and subcellular localization analyses of the transcription factors SKN-1, HLH-30, and DAF-16 indicate their functional interplay. The observed coordinated activation of these evolutionarily conserved regulators of longevity supports the hypothesis of a multimodal mechanism of action through which PGL enhances stress resistance and promotes lifespan extension in *C. elegans*.

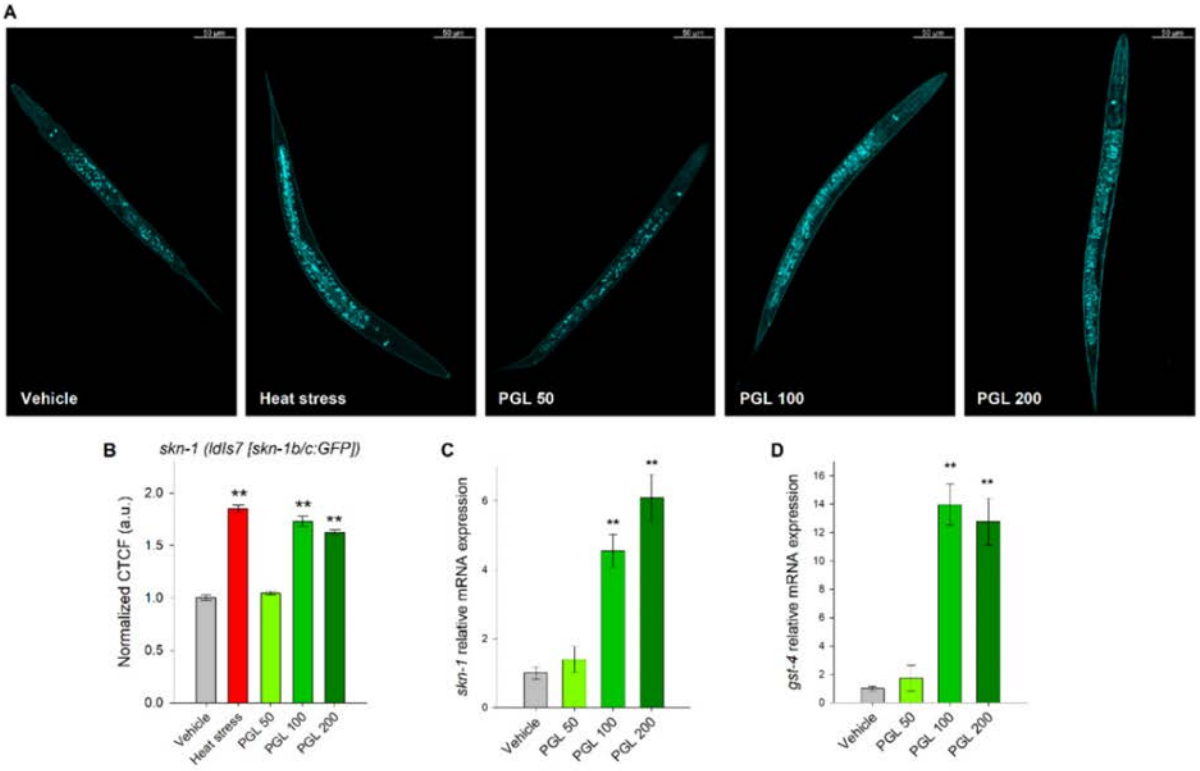

Figure 12. Effect of PGL extract on SKN-1::GFP subcellular distribution, *skn-1* mRNA expression and it downstream target *gst-4*. (A) Representative fluorescent confocal microphotographs at 20x magnification (scale bar of 50 μm) of vehicle, heat-stressed control (37 °C for 5 min) or PGL-treated (50, 100 and 200 μg/ml) *C. elegans* LD1 *ldIs7* [*skn-1b/c*::*GFP* + *rol-6*(*su1006*)]. (B) Cell total correlates fluorescence (CTCF), normalized and compared to the vehicle group, ± SEM, $n = 60$, $^{**}p < 0.01$, (one-way ANOVA). Normalized relative mRNA expression levels of *skn-1* (C), and *gst-4* (D) upon treatment with vehicle or PGL extract. Data are expressed as mean ± SEM, $n = 9$, $^{*}p < 0.05$ and $^{**}p < 0.01$ compared to the vehicle group (one-way ANOVA).

2.7 Effect of PGL treatment on mitochondrial function

With advancing age, many organisms exhibit reduced mitochondrial integrity, characterized by impaired mitochondrial biogenesis, increased accumulation of damage, and decreased mitochondrial membrane potential (ΔΨm). Maintenance of balanced mitochondrial mass and stable ΔΨm is considered a key molecular determinant of cellular health and longevity (Tyshkovskiy et al., 2023).

To evaluate the effects of pomegranate leaf extract on mitochondrial status, functional assays were performed using the fluorescent dyes TMRE and MVG. The results demonstrated

that PGL treatment induced a dose-dependent increase in mitochondrial mass (Fig. 23A, B), along with a significant elevation of ΔΨm (Fig. 23A, C) compared to the control group.

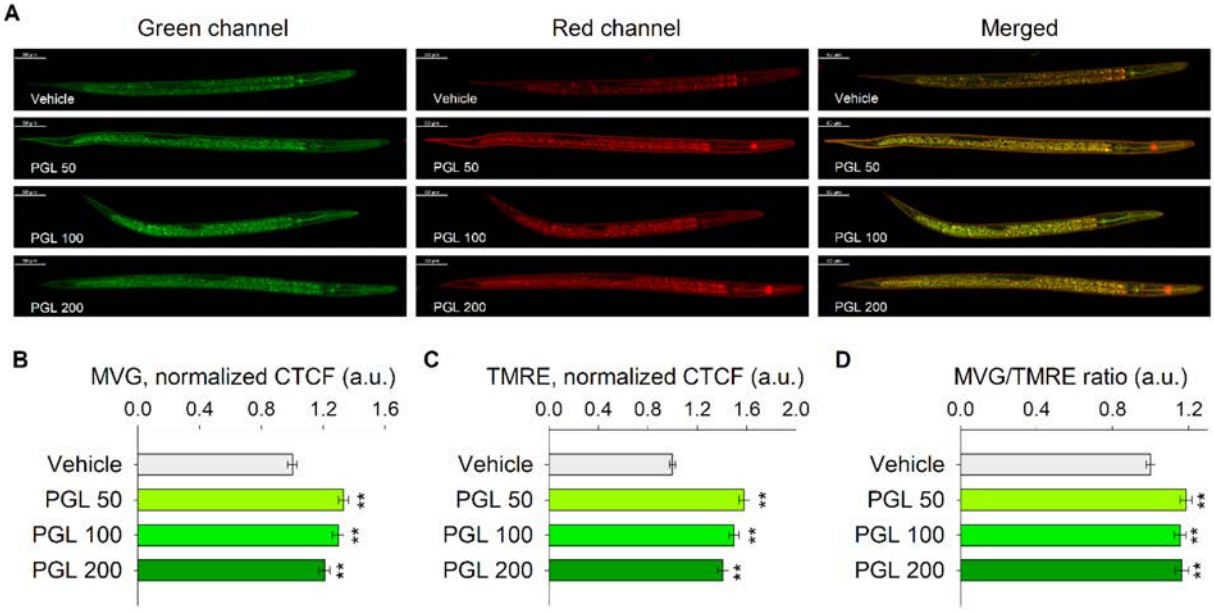

Figure 13. Effect of PGL extract on mitochondrial integrity and dynamics (A) Representative fluorescent confocal microphotographs at 20x magnification (scale bar of 50 μm) of green and red channel, and merged image of vehicle or PGL-treated *C. elegans* co-stained with MVG and TMRE. (B) Cell total correlates fluorescence (CTCF) of MVG, normalized to the vehicle. (C) Normalized CTCF of TMRE fluorescent intensity, normalized to the vehicle. (D) Ratio of TMRE to MVG whole-body fluorescence demonstrating increased mitochondrial membrane potential relative to mitochondrial mass in response to PGL treatment. The data are shown as means ± SEM, $n = 60$, $^{**}p < 0.01$, compared to the vehicle (one-way ANOVA).

The observed effects on mitochondrial function are consistent with previous findings of increased *hlh-30*/TFEB expression and downregulation of *let-363*/mTOR (Fig. 19C, E), supporting their involvement in the regulation of mitochondrial integrity and biogenesis mediated by the extract.

These data highlight the potential of PGL to exert protective effects on the mitochondrial network, thereby contributing to the maintenance of cellular energy homeostasis under ageing conditions.

3. Evaluation of the potential of *P. granatum* juice as a functional food with geroprotective effects

Pomegranate fruits have long been used as a “medicinal food” in various cultures and traditional medical systems for the treatment of infections, fever, ulcers, diarrhea, aphthae, acidosis, hemorrhages, dysentery, and respiratory disorders (Maphetu et al., 2022). Owing to their rich content of secondary metabolites, pomegranate juice exhibits a broad spectrum of pharmacological activities, including anti-inflammatory and neuroprotective effects (Bahari et al., 2023; Moradnia et al., 2024).

Furthermore, pomegranate fruits and their derived juice are considered contributors to the health benefits of the Mediterranean diet, a dietary pattern strongly associated with longevity and extended healthspan (Moradnia et al., 2024). Despite these well-documented health-promoting properties, pomegranate juice remains insufficiently explored in the context of its potential to modulate ageing processes.

3.1. Analysis of physiological parameters and lifespan

As an initial step in evaluating the potential of pomegranate juice to modulate ageing, a viability assay was performed to determine optimal treatment concentrations. The juice was added to heat-inactivated, 10× concentrated *E. coli* OP50 to achieve final concentrations ranging from 10 to 200 µg/mL. Treatment was carried out for 48 h during the L1–L4 larval stages.

No significant effects on viability were observed at any of the tested concentrations compared to the control group (Fig. 24A). Based on these findings, concentrations of 50, 100, and 200 µg/mL were selected for subsequent experiments.

Locomotor activity, assessed by the rate and/or number of body bends, is a well-established indicator of physiological status and neuromuscular function in *Caenorhabditis elegans* (Chen X. et al., 2024; Son et al., 2019). Movement reflects the coordinated activity of dorsal and ventral musculature and serves as a robust age-dependent marker (Spanoudakis and Tavernarakis, 2023).

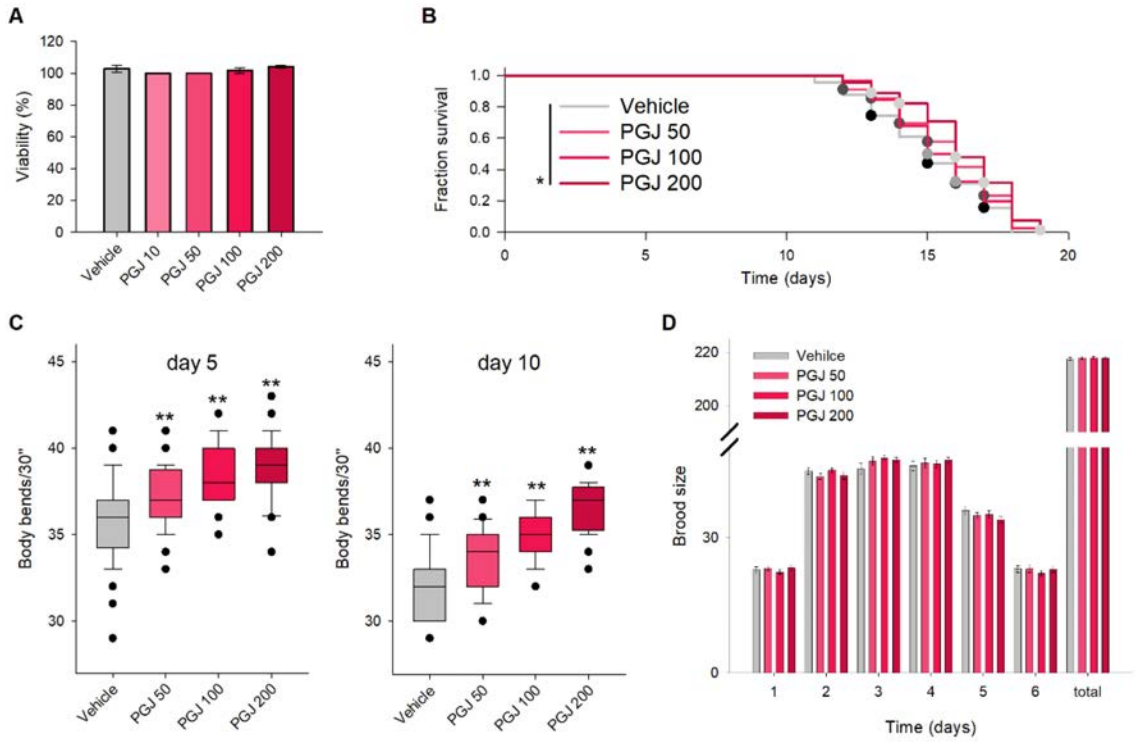

Figure 14. Pomegranate juice (PGJ) improves locomotor activity and extends lifespan in *C. elegans*. (A) Viability assay following treatment with PGJ at concentrations of 10–200 μg/mL. (B) Lifespan analysis of nematodes treated with PGJ at concentrations of 50, 100, and 200 μg/mL. Lifespan, expressed as survival fraction, was compared between PGJ-treated and control groups using Kaplan–Meier survival curves (n = 90). Statistical significance was determined using the log-rank test. (C) Locomotor activity measured as body bends per 30s on days 5 and 10 of adulthood (n = 45). (D) Daily and total progeny of PGJ-treated nematodes (n = 15). Data in panels (A, C, and D) are presented as mean ± SEM. Statistical significance: $p < 0.05$, $p < 0.01$ vs. control group (ANOVA).

Treatment with pomegranate juice at the selected concentrations resulted in a statistically significant and dose-dependent increase in locomotor activity in both young (day 5) and aged nematodes (day 10; Fig. 24C). In young individuals, this effect may be associated with enhanced metabolic efficiency, in line with previous studies linking pomegranate juice consumption to mitochondrial activation and increased energy expenditure (Maphetu et al., 2022). In contrast, the preservation of locomotor function in aged worms may reflect a potential neuroprotective effect (Fahmy et al., 2020).

With respect to longevity, a statistically significant increase in lifespan was observed only at the highest tested concentration of 200 μg/mL (Fig. 24B).

Reproductive capacity was also evaluated, including both total progeny over the reproductive period and its daily distribution. The results showed no statistically significant changes in brood size compared to the control group (Fig. 24D), further supporting the absence of toxicity at the tested concentrations.

In summary, phenotypic analyses indicate that *P. granatum* juice has the potential to support physiological parameters associated with healthy ageing by enhancing locomotor activity and preserving reproductive function, while a significant lifespan-extending effect was observed at 200 μg/mL.

3.2. Effect of PGJ on stress response

Enhanced resistance to stressors is a well-established marker of healthy ageing, as it is closely associated with the activation of cellular defense mechanisms and the maintenance of homeostasis (Banse et al., 2024; Dues et al., 2016; Hetz et al., 2020).

In addition to locomotor activity and reproductive capacity, the effects of PGJ on stress resistance, both oxidative and thermal, were also evaluated (Fig. 25B).

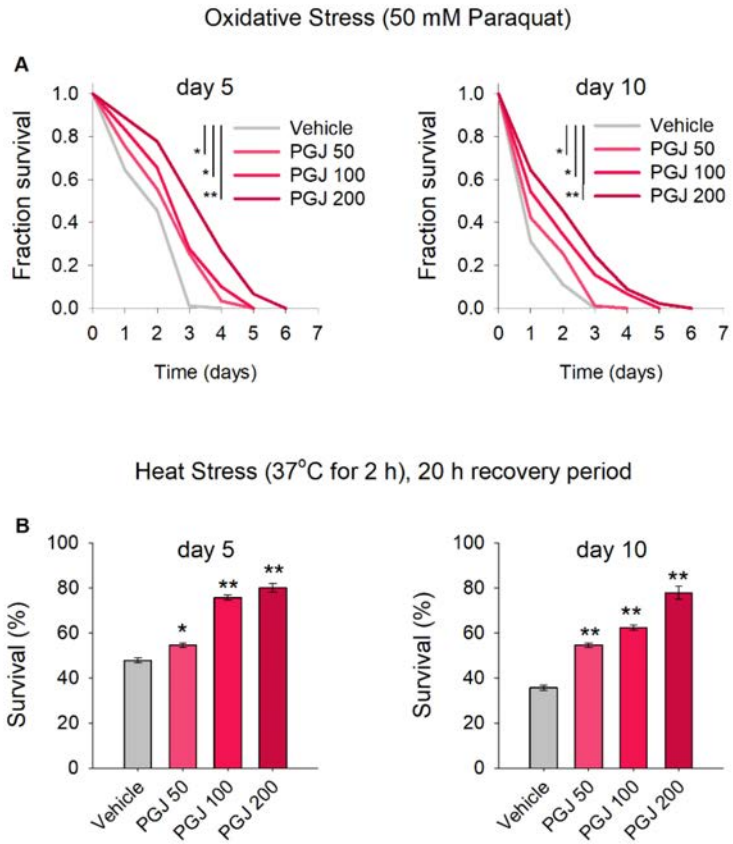

Figure 15. Pomegranate juice (PGJ) enhances resistance to oxidative and thermal stress. Wild-type N2 nematodes were treated with PGJ at concentrations of 50, 100, and 200 μg/mL or with vehicle (0.2% DMSO). (A) Survival curves under oxidative stress induced by paraquat (50 mM), monitored at 24 h intervals in N2 nematodes. Data were analyzed using Kaplan–Meier survival analysis, and statistical significance was determined by the log-rank test ($p < 0.05$, $p < 0.01$). (B) Survival following acute thermal stress (37 °C for 2 h), followed by a 20 h recovery period under standard conditions, and assessed on days 5 and 10 of adulthood. Results are presented as percentage survival (mean ± SEM, $n = 90$), with statistical significance indicated as $p < 0.05$, $p < 0.01$ (ANOVA).

The assays were conducted in both young (day 5) and aged (day 10) individuals. Upon exposure to acute thermal stress (37 °C for 2 h), nematodes treated with pomegranate juice exhibited significantly higher survival compared to untreated controls, in both age groups (Fig. 25B).

Similar results were observed under acute oxidative stress induced by methyl viologen (50 mM). On day 5, PGJ-treated worms showed a dose-dependent increase in both mean and maximum survival relative to controls (Fig. 25A). Although the effect was less pronounced in aged individuals (day 10), a consistent trend toward improved stress resistance was maintained.

In summary, these findings demonstrate that, in addition to improving locomotor function and preserving reproductive capacity, pomegranate juice enhances resistance to cellular stress in both young and aged nematodes. This supports its potential as a natural agent for maintaining physiological resilience during ageing, even in the absence of a direct lifespan-extending effect.

4. Evaluation of the effects of ADAPT-232 on lifespan and mitochondrial function

Plant adaptogens are well studied for their ability to enhance stress resistance, including through modulation of the sympathetic nervous system and maintenance of physiological homeostasis (Panossian et al., 2021; Tóth-Mészáros et al., 2023). However, their role as potential modulators of ageing processes and mitochondrial function remains relatively underexplored, particularly when administered as combined formulations.

The present study aimed to evaluate the effects of the standardized and chemically well-characterized adaptogenic formulation ADAPT-232, containing extracts from *Rhodiola rosea*,

Schisandra chinensis, and *Eleutherococcus senticosus*, on lifespan, molecular markers of ageing, and mitochondrial integrity in the model organism *C. elegans*.

4.1. Phenotypic analysis, stress resistance, and morphological assessment

The chemically defined formula ADAPT-232, comprising extracts of *R. rosea*, *S. chinensis*, and *E. senticosus*, represents a mixture of adaptogens with well-documented beneficial effects on health, particularly in the context of physical endurance and cognitive performance (Tóth-Mészáros et al., 2023). Based on the available literature and preliminary data, three experimental concentrations (50, 100, and 200 μg/mL) were selected for the current study.

Lifespan analysis demonstrated that ADAPT-232 dose-dependently modulates ageing and promotes longevity (Fig. 26D), with the most pronounced effect observed at the highest concentration of 200 μg/mL.

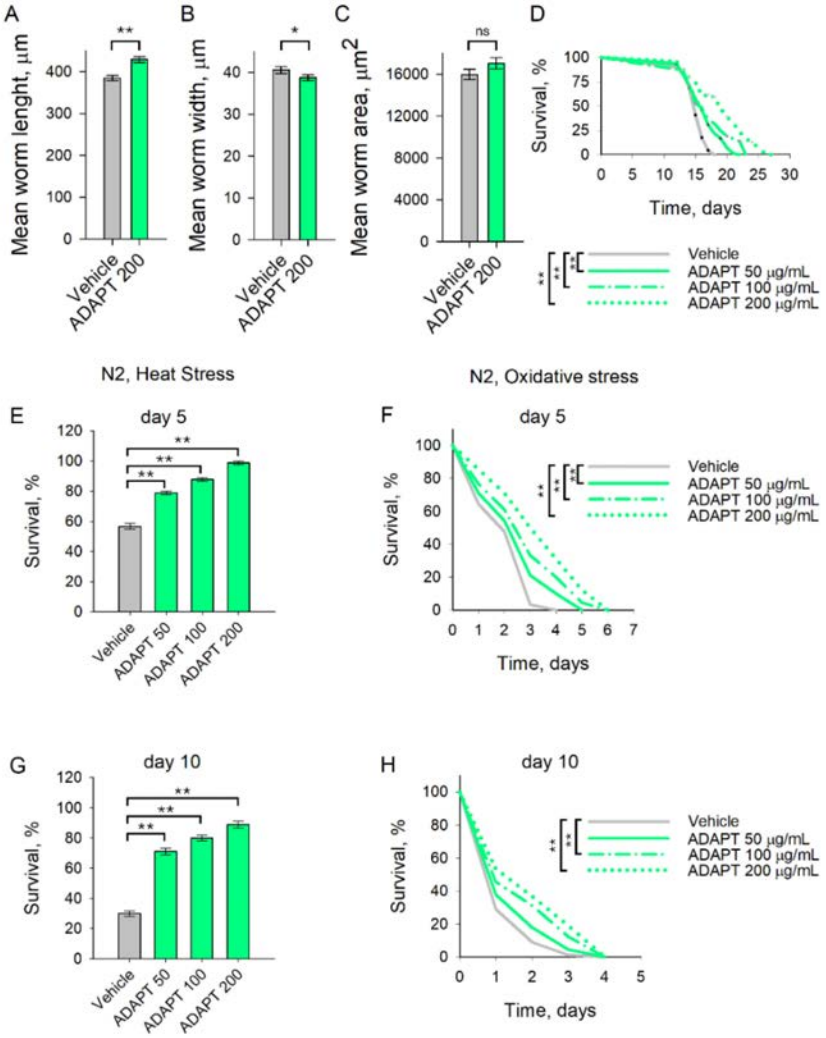

Figure 16. Treatment with ADAPT-232 extends lifespan, enhances resistance to thermal and oxidative stress, and modulates body morphology in *C. elegans*. Wild-type nematodes

were pre-treated with ADAPT-232 at concentrations of 50, 100, or 200 μg/mL during the L3–L4 larval stages. Body morphology was analyzed using the automated tracking system WormLab, assessing (A) mean body length, (B) width, and (C) body area. Data are presented as mean ± SEM (n = 100–150); ns, not significant; $p < 0.05$, $p < 0.01$ (Mann–Whitney rank-sum test). Survival following thermal stress (37 °C) was evaluated on (E) day 5 and (G) day 10 of adulthood. Survival under acute oxidative stress (50 mM methyl viologen) was assessed on (F) day 5 and (H) day 10. (E, G) Thermal stress results are presented as percentage survival (mean ± SEM, n = 90); statistical analysis was performed using ANOVA ($p < 0.05$, $p < 0.01$ vs. vehicle group). (F, H) Survival under oxidative stress was monitored at 24 h intervals until complete lethality. Data were analyzed using Kaplan–Meier survival analysis, with statistical significance determined by the log-rank test ($p < 0.05$, $p < 0.01$; n = 90).

Statistically significant changes in body morphology were also observed in *C. elegans* following treatment with ADAPT-232 (Fig. 26A–C), characterized by increased body length (Fig. 26A) and reduced body width (Fig. 26B), resulting in an overall increase in body area compared to the control group (Fig. 26C).

These findings are consistent with previous reports indicating that extracts from plants included in ADAPT-232, such as *Rhodiola rosea*, can extend lifespan in preclinical models, including *C. elegans* (Jiang et al., 2021; Teng et al., 2022).

Based on the lifespan data and the observed potential of ADAPT-232, its effect on survival under acute cellular stress induced by high temperature was further evaluated in both young and aged individuals.

The results demonstrate that the adaptogenic formulation significantly improves thermotolerance at all tested concentrations (Fig. 26E, G). A similar trend was observed under exposure to 50 mM paraquat (Fig. 26F, H), with ADAPT-232-treated nematodes exhibiting reduced sensitivity to oxidative damage.

4.2. Analysis of key longevity-assosiated transcription factors

The transcription factors DAF-16 and SKN-1 play central roles in regulating genes involved in cellular stress responses, metabolic homeostasis, and ageing and longevity in *C. elegans*. Their nuclear translocation is a well-established marker of functional activation and indicates engagement of endogenous protective mechanisms (Jiang et al., 2021; Lin et al., 2018; Sen et al., 2020).

To determine whether ADAPT-232 induces activation of DAF-16 and SKN-1, confocal microscopy analysis was performed using GFP-labeled transgenic nematode lines: OH16024 *daf-16* [ot971(*daf-16*::GFP) I] и LD1 [*skn-1b/c*::GFP].

The results revealed induction of nuclear localization of DAF-16 at concentrations of 100 and 200 μg/mL (Fig. 27A). Similarly, a marked increase in GFP signal intensity was observed for SKN-1 compared to the control group, confirming activation of this regulatory pathway (Fig. 27C). To further validate these findings, mutant strains lacking functional DAF-16 and SKN-1 were examined. In contrast to wild-type worms, no lifespan extension was observed in these mutants following ADAPT-232 treatment (Fig. 27B, D), supporting the conclusion that the beneficial effects of ADAPT-232 are mediated through activation of DAF-16 and SKN-1.

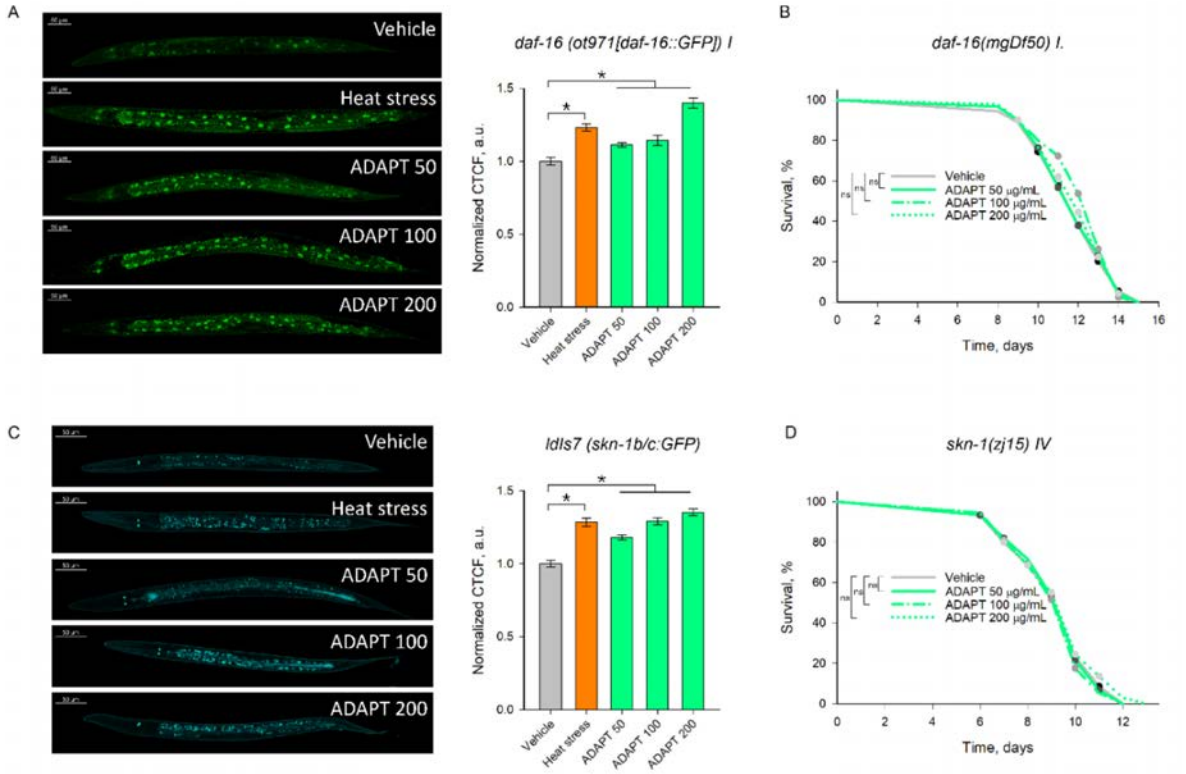

Figure 17. The formula ADAPT-232 induces the nuclear translocation of DAF-16 и a SKN-1/NRF2. Coordinated SKN-1 and DAF-16 signalling mediates ADAPT-232-induced healthspan extension. Representative fluorescent confocal microphotographs at 20 × magnification (scale bar of 50 μm) and quantification of the fluorescence of vehicle, heat-stressed control (37 °C for 5 min) or ADAPT-232-treated (50, 100, or 200 μg/ml) *C. elegans* strains – (A) OH16024 *daf-16* [*ot971*(daf-16::GFP) I] and (C) LD1 *ldIs7* [skn-1b/c::GFP + rol-6(su1006)] represented as cell total correlated fluorescence (CTCF), normalized and compared to the vehicle group, ± SEM, n = 60, *p < 0.05, (ANOVA on ranks). Survival curves form Kaplan Mayer of loss of function mutant strains for (B) DAF-16 (GR1307 *daf-16*(mgDf50) I.)

and (D) SKN-1 (QV225 *skn-1*(zj15) IV.), presented as Kaplan-Meier survival curves, and analysed by the log-rank test, ns – not significant.

The observed correlation between the activation of the two transcription factors and the demonstrated enhancement of stress resistance and physiological function suggests that ADAPT-232 exerts its effects through coordinated stimulation of endogenous protective mechanisms. This is consistent with the concept of multimodal adaptogenic action and highlights the potential of the combined formulation to modulate ageing processes.

4.3. Effects of ADAPT-232 on impaired lipid metabolism

Ageing is accompanied by significant metabolic alterations, including impaired glucose homeostasis, increased insulin resistance, and dysregulation of lipid metabolism (Lara-Castor et al., 2025). In this context, a model of induced metabolic dysfunction in *C. elegans* was employed by supplementing the growth medium with 2% glucose. Exposure to high glucose levels resulted in pronounced lipid accumulation, visualized by fluorescence microscopy following Nile Red staining, a widely used method for assessing neutral lipid stores (Zong et al., 2024).

Treatment with ADAPT-232 (50, 100, and 200 μg/mL) led to a statistically significant reduction in triglyceride levels compared to the glucose control group (Fig. 28A). This effect indicates decreased lipid accumulation and suggests improved metabolic regulation. To validate these findings, a colorimetric quantification of triglycerides was also performed, confirming that all tested concentrations of ADAPT-232 significantly reduced triglyceride levels (Fig. 28B).

The modulation of lipid metabolism likely represents part of an integrated cellular response induced by the formulation, aimed at maintaining metabolic homeostasis under stress conditions.

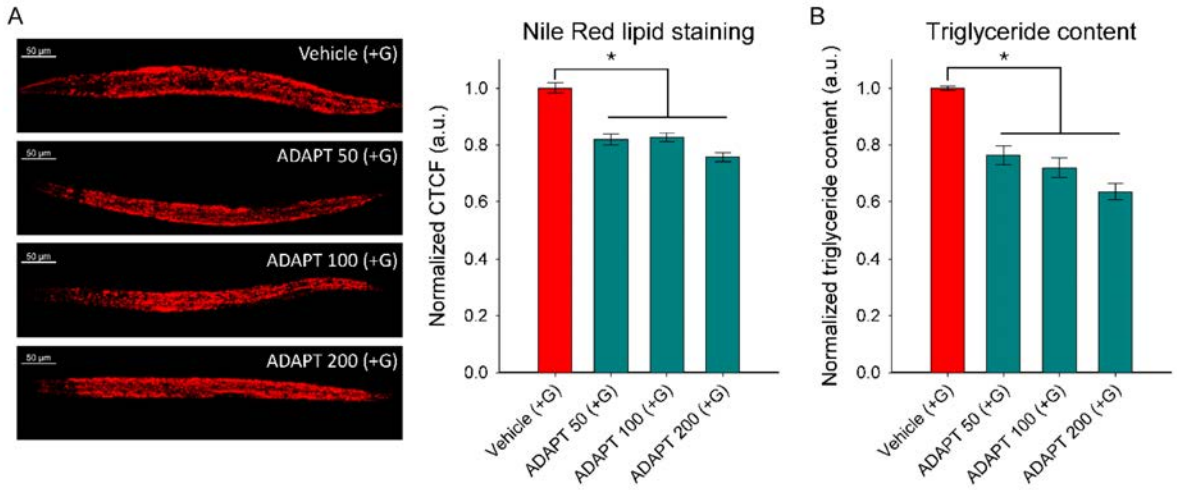

Фигура 28. The combined formula ADAPT-232 reduces lipid accumulation in *C. elegans*. (A) Representative confocal images of Nile Red-stained lipids in a model of glucose-induced lipid accumulation in *Caenorhabditis elegans* following 24 h treatment with 50, 100, or 200 μg/mL ADAPT-232 or vehicle (0.2% DMSO). (B) Quantification of lipid accumulation, expressed as corrected total cell fluorescence (CTCF), and (C) normalized triglyceride content, expressed in arbitrary units (a.u.). Data are presented as mean ± SEM; $p^* < 0.05$ compared to vehicle group (+G) (ANOVA).

4.4. Effects of ADAPT-232 on mitochondrial dysfunction

In addition to promoting lipid accumulation, glucose supplementation in *C. elegans* is a well-established approach for modeling mitochondrial dysfunction. Elevated glucose levels lead to reduced mitochondrial efficiency, decreased membrane potential, and impaired energy homeostasis, all of which hallmarks of metabolic syndrome, type 2 diabetes, and age-related degenerative conditions (Mao et al., 2019; Zong et al., 2024).

To assess the potential effects of ADAPT-232 on mitochondrial function, fluorescence-based analyses were conducted using specific dyes, namely MVG to label mitochondrial mass and TMRE to assess mitochondrial membrane potential (Fig. 29A, B). In *C. elegans*, mitochondrial dysfunction triggers a cascade of protective responses, with pronounced alterations observed in intestinal mitochondria, which become redistributed toward the lumen of intestinal cells (Mao et al., 2019; Onraet et al., 2023).

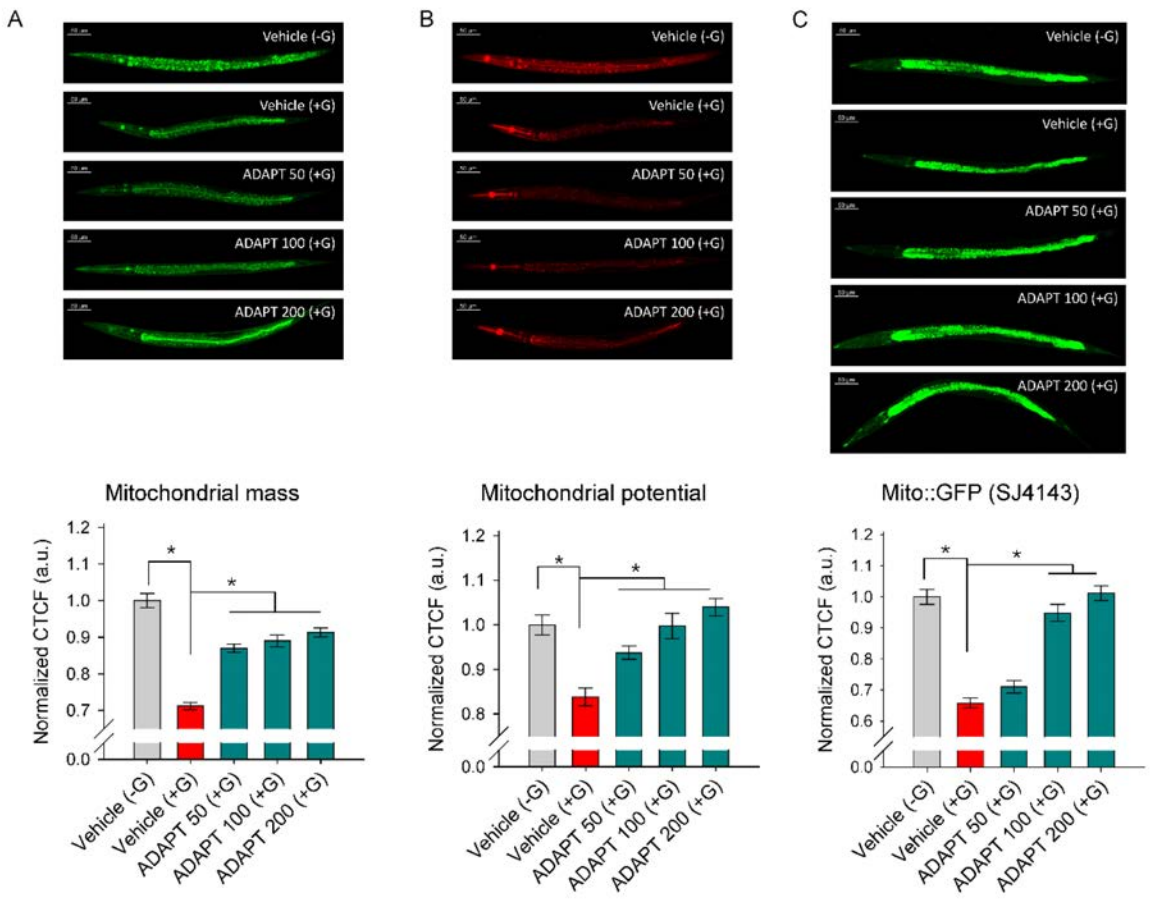

Figure 19. ADAPT-232 restores mitochondrial mass and membrane potential in a model of mitochondrial dysfunction and improves energy distribution in the intestine of the SJ4143 strain. Representative confocal images and corresponding corrected total cell fluorescence (CTCF), normalized to the control group (−G), are shown for: (A) N2 nematodes stained with MVG, (B) N2 nematodes stained with TMRE, and (C) SJ4143 strain nematodes treated for 24 h with 50, 100, or 200 μg/mL ADAPT-232 or vehicle, in the presence (+G) or absence (−G) of glucose.

In addition to the assessment of mitochondrial mass and membrane potential, mitochondrial responses were evaluated in the transgenic nematode strain SJ4143, which expresses GFP-labeled mitochondria localized in intestinal cells (Fig. 29C). The use of this strain provides valuable insight into both intestinal mitochondrial mass and activity, thereby offering a comprehensive view of energy metabolism within intestinal tissue.

The results demonstrated that a glucose-enriched diet led to a statistically significant reduction in fluorescence intensity compared to the control group, confirming the presence of mitochondrial dysfunction (Fig. 29A–C). Supplementation with ADAPT-232 under glucose

conditions restored fluorescence levels to values comparable to those observed under normal conditions (Fig. 29A–C), with the effect being statistically significant relative to the glucose-treated group.

These findings support the hypothesis that ADAPT-232 exerts a protective effect on intestinal mitochondrial function by counteracting glucose-induced mitochondrial impairment.

VI. DISCUSSION

In contemporary biomedical science, ageing is recognized as a major risk factor for the development of chronic non-communicable diseases and a primary driver of the progressive decline in quality of life (López-Otín et al., 2013, 2023; Shen et al., 2024). In the context of global population ageing, there is an increasing need to develop effective strategies for the prevention and modulation of ageing at the cellular and molecular levels (Chen et al., 2018, 2025; Liu et al., 2025).

One of the most promising approaches for delaying ageing processes is the use of plant-derived natural products as a source of structurally diverse secondary metabolites (Longo and Anderson, 2022; Thomas et al., 2023). Although numerous natural products have been investigated in the context of various pathological conditions, their systematic exploration as potential geroprotective agents remains a rapidly evolving field (Fahey et al., 2021; Guo et al., 2022).

The present dissertation implements an integrative approach that combines ethnopharmacological selection of plant-derived natural products with functional and molecular analyses aimed at evaluating their potential to modulate evolutionarily conserved ageing mechanisms.

The investigated interventions span multiple levels of phytochemical complexity from bioactive compounds (icariin), through plant extracts (*P. granatum* leaf), to functional foods (juice from *P. granatum* fruits) and a standardized combined formulation (ADAPT-232). This approach enables the assessment of both individual compounds and complex phytochemical mixtures in relation to key processes underlying physiological ageing and longevity.

1. Icariin enhances stress resistance and extends lifespan in *C. elegans* through an *hsf-1*- and *daf-2*-mediated hormetic response

The results of the present study demonstrate that icariin induces lifespan extension in wild-type *C. elegans* (N2), whereas this effect is not observed in *daf-2* mutants, highlighting the critical

role of the insulin/IGF-1 signaling (IIS) pathway in its mechanism of action. In addition to increased lifespan, icariin-treated nematodes exhibit improved locomotion, enhanced resistance to both thermal and oxidative stress, and significantly reduced lipid accumulation.

The observed combination of increased stress resistance and improved motor function is indicative of a hormetic mode of action. This principle underlies several well-established lifespan-extending interventions, including caloric restriction, intermittent fasting, and controlled exposure to mild stressors (Matai et al., 2019; Shaposhnikov et al., 2022).

More specifically, HSF-1, a master regulator of the heat shock response and proteostasis, is activated by icariin at higher concentrations, consistent with its established role as a key mediator of hormesis (Tan et al., 2022; Xu et al., 2023). Similar responses have been reported for other bioactive compounds with hormetic properties, such as resveratrol, quercetin, and sulforaphane (Martel et al., 2019).

Icariin exhibits a pronounced dose-dependent hormetic effect, with 50 μM identified as the optimal concentration for inducing coordinated regulation of DAF-16 and SKN-1. At this dose, nuclear translocation of DAF-16 is observed, along with increased expression of *sir-2.4* and *jnk-1*, both key regulators of stress signaling and autophagy-related processes (Hansen et al., 2018; Lin et al., 2018; Tuohetaerbaike et al., 2020). At the higher concentration (100 μM), the mechanism shifts predominantly toward HSF-1 activation, while the activity of other pathways is markedly reduced. This represents a classic example of dose-dependent bimodality characteristic of hormetic responses (Jodynis-Liebert et al., 2020; Xu et al., 2022).

Based on these findings, a schematic model summarizing the molecular mechanism of action of icariin—linked to hormetic response and lifespan extension—is presented (Fig. 30).

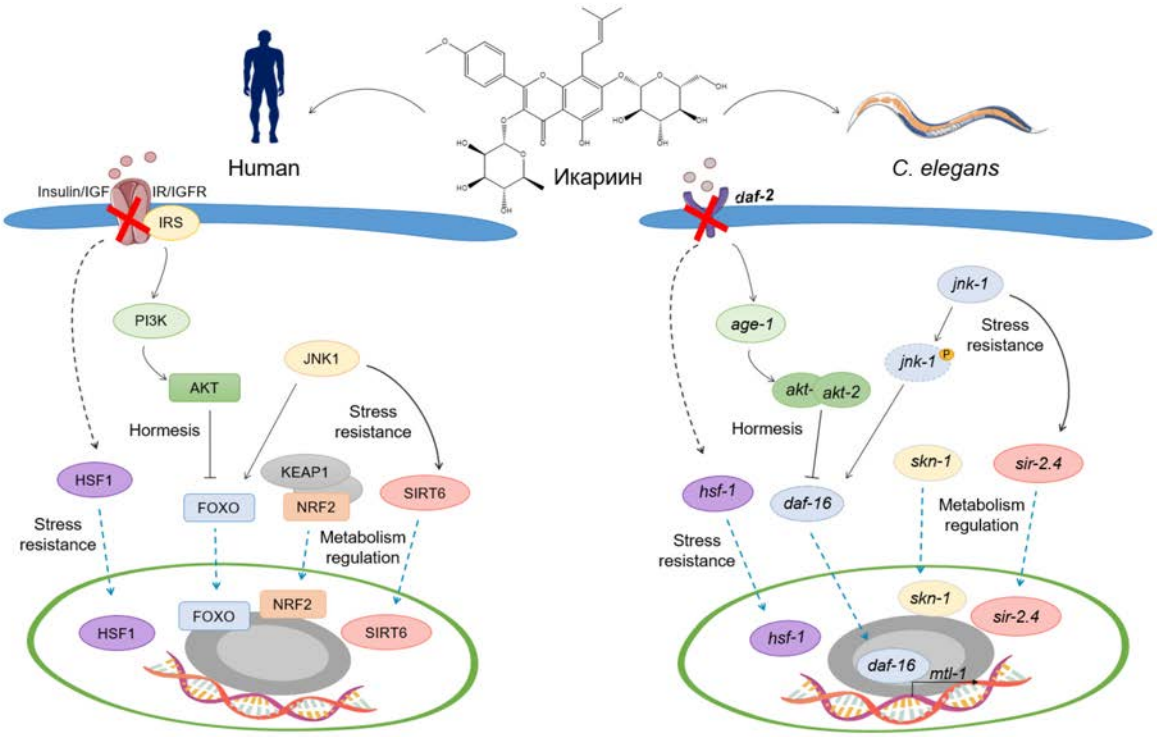

Figure 20. Proposed mechanism of action illustrating evolutionarily conserved molecular mediators underlying the hormetic effects of icariin in *Caenorhabditis elegans*. At a concentration of 50 μM, icariin suppresses *daf-2*/IGF, a key component of the insulin/IGF-1 signaling (IIS) pathway. This leads to activation of the transcription factor DAF-16/FOXO, which translocates to the nucleus and induces the expression of the metallothionein *mtl-1*, involved in cellular protection against oxidative stress. Under stress conditions, activation of *jnk-1*/JNK1 facilitates the nuclear translocation of DAF-16 and contributes to the activation of *sir-2.4*/SIRT6. Treatment with 50 μM icariin also upregulates *skn-1*/NRF2 expression, likely contributing to improved cellular homeostasis. Notably, activation of *hsf-1*/HSF1 is observed at all tested concentrations of icariin, placing it at the center of the observed lifespan-extending effects. As a key regulator of proteostasis, HSF-1 likely plays a pivotal role in mediating the beneficial effects of icariin on longevity.

2. The *P. granatum* leaf extract promotes longevity through coordinated interaction of HLH-30/TFEB, DAF-16/FOXO, and SKN-1/NRF2 signaling pathways

In the present study, treatment with *P. granatum* leaf extract (PGL) significantly improves locomotor activity and fertility in *Caenorhabditis elegans*, with the observed effects likely associated with enhanced mitochondrial integrity. Age-related decline in locomotion is often

linked to mitochondrial dysfunction; therefore, its restoration by PGL suggests a beneficial impact on cellular energy homeostasis (Daskalaki et al., 2023; Spanoudakis and Tavernarakis, 2023).

Analysis of metabolic parameters revealed that PGL modulates basal metabolism, as evidenced by reduced lipid accumulation in *C. elegans*. This effect is accompanied by increased expression of the transcription factor *hlh-30*/TFEB and decreased expression of *let-363*/mTOR, both key regulators of autophagy. Furthermore, data obtained from oxidative stress experiments using the double mutant strain MIR-13, characterized by impaired *aak-2* and *sir-2.1* function, confirm the functional importance of this axis in stress protection, as PGL fails to restore stress resistance under conditions of reduced *aak-2* and *sir-2.1* activity.

PGL treatment induces increased expression and nuclear translocation of the transcription factors DAF-16/FOXO and HLH-30/TFEB, indicating activation of cellular pathways associated with lifespan extension and maintenance of proteostasis. Interestingly, although an increase in *daf-2* expression is observed, which would typically suggest IIS activation and DAF-16 inhibition, the effect on DAF-16 is paradoxically activating. This may be explained by an alternative regulatory mechanism, likely involving inhibition of mTOR signaling. This hypothesis is further supported by the concurrent upregulation of *skn-1*/NRF2 and its downstream target *gst-4*, confirming activation of antioxidant defense pathways.

The observed increase in mitochondrial mass and membrane potential ($\Delta\Psi m$) following PGL treatment suggests enhanced mitochondrial biogenesis and function, likely resulting from the coordinated regulation of *hlh-30* and *let-363*. This effect is associated with improved cellular respiration, enhanced energy efficiency, and increased resistance to age-related degenerative processes, including immune responses mediated by the *sek-1*/PMK-1/p38 MAPK pathway.

Collectively, these findings define the molecular basis of the biological activity of *P. granatum* leaf extract and provide strong evidence that PGL activates evolutionarily conserved pathways involved in stress response, metabolic adaptation, and longevity regulation in *C. elegans*.

The most significant conclusion of this study is that HLH-30/TFEB emerges as a central regulatory node in the mechanism of action of PGL, coordinating metabolic, antioxidant, and stress-response pathways. These results highlight the potential of *P. granatum* leaf extract as a natural intervention for delaying ageing and promoting healthy lifespan.

A schematic model summarizing the proposed mechanism of action is presented in Figure 21.

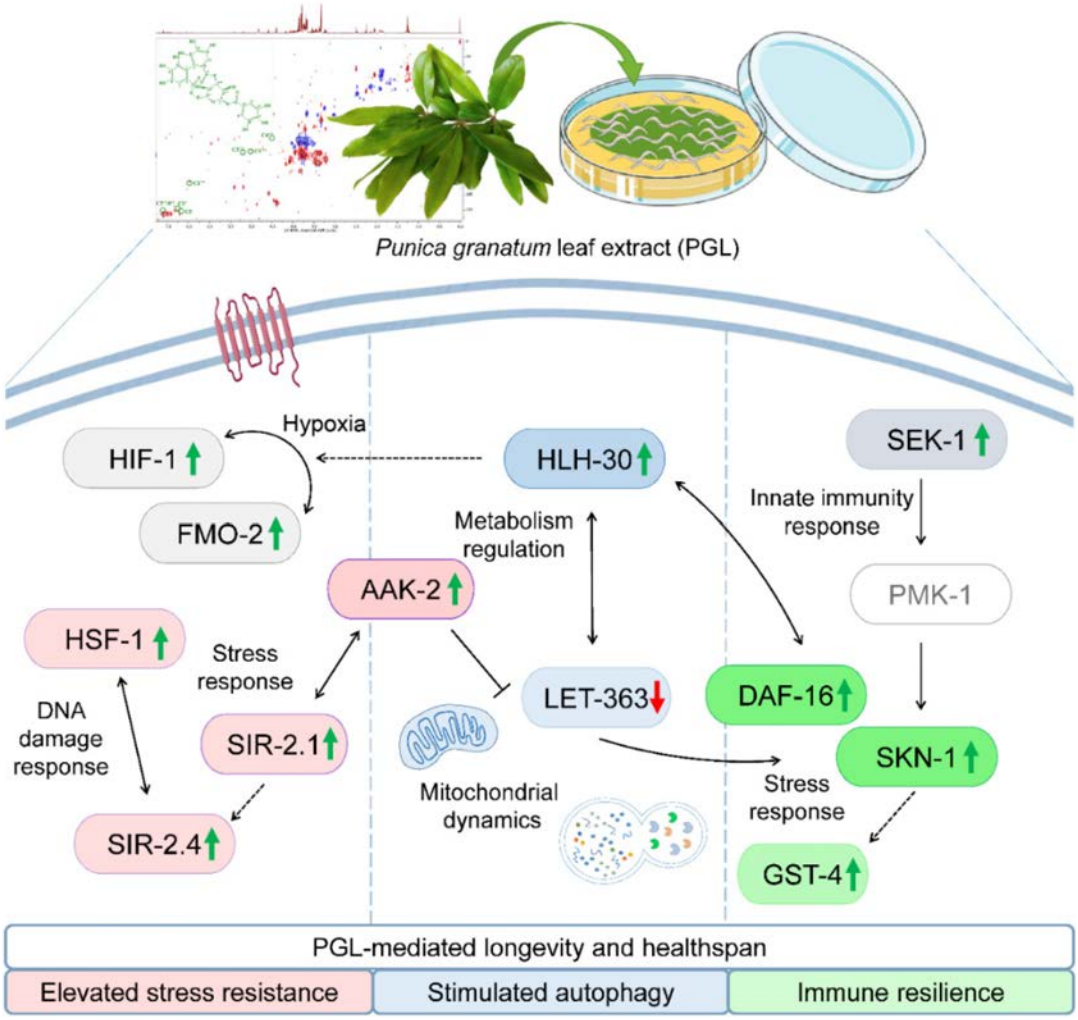

Figure 21. Molecular mechanism underlying the effects of *P. granatum* leaf extract (PGL) on the longevity-associated signaling network in *Caenorhabditis elegans*. Treatment with PGL activates a cascade of molecular events aimed at enhancing cellular resilience and metabolic homeostasis. The transcription factor HLH-30 is activated in response to PGL and mediates the expression of genes associated with hypoxia response, including *hif-1* and *fmo-2*, thereby promoting stress adaptation. Concurrently, HLH-30 interacts with LET-363/mTOR, contributing to improved metabolic regulation and increased mitochondrial membrane potential (ΔΨm). In addition, *let-363* modulates the activity of DAF-16/FOXO and SKN-1/NRF2, while *sek-1*, as part of innate immune signaling, induces activation of *pmk-1*, which in turn promotes the expression of SKN-1 and its downstream target *gst-4*. Furthermore, co-activation of *aak-2*/AMPK and *sir-2.1*/SIRT1 enhances the response to oxidative stress, while

HSF-1 and SIR-2.1 act synergistically to promote DNA damage repair mechanisms. Collectively, these interactions highlight the multimodal effects of PGL treatment and its potential to modulate longevity through evolutionarily conserved molecular pathways.

3. Supplementation with *P. granatum* juice improves age-related physiological decline and modulates stress response

The results of the present study demonstrate that pomegranate juice extends lifespan in *C. elegans* only at the highest tested concentration (200 μg/mL) compared to the control group. A significant increase in locomotor activity is also observed in both young and ageing individuals, indicating improved neuromuscular function. This finding is consistent with previous studies reporting the neuromodulatory and neuroprotective potential of pomegranate juice and its bioactive components in experimental models of Alzheimer's and Parkinson's diseases (Chen P. et al., 2025; Eghbali et al., 2021; Maphetu et al., 2022).

In addition, the enhanced locomotor activity may be associated with increased energy efficiency and improved mitochondrial function. This is in line with reports linking pomegranate juice consumption to beneficial effects in metabolic disorders such as obesity and type 2 diabetes, mediated through stimulation of mitochondrial activity and optimization of energy metabolism (Bahari et al., 2024; Banihani et al., 2019).

The increased stress resistance observed following pomegranate juice treatment likely represents a key mechanism underlying its beneficial effects on organismal health.

In conclusion, the findings of this study demonstrate that pomegranate juice enhances lifespan in *C. elegans* (at higher concentrations) and improves functional parameters associated with healthy ageing. The observed increases in locomotor activity and stress resistance further support its positive impact on overall physiological condition.

4. The combined formulation ADAPT-232 delays ageing processes and improves mitochondrial function through regulation of DAF-16 and SKN-1

In the present study, the combined formulation ADAPT-232 was shown to significantly extend lifespan, which at the molecular level correlates with enhanced activation of DAF-16 and SKN-1. These findings suggest that these transcription factors act as central mediators of both the health-promoting effects of the formulation and its underlying mechanism of action.

The results further demonstrate that ADAPT-232 exerts a multifaceted effect on healthspan by improving metabolic and mitochondrial homeostasis, stimulating lipid

catabolism, and supporting mitochondrial quality control, largely through the coordinated activation of DAF-16 and SKN-1. These data provide a mechanistic basis for the potential of ADAPT-232 to counteract mitochondrial dysfunction and highlight its promise as a supportive intervention in ageing- and metabolism-related disorders.

In addition, the present study shows that ADAPT-232 effectively reduces triglyceride levels in a model of glucose-induced lipid accumulation in *C. elegans*. This observation is consistent with previous reports demonstrating that *Rhodiola rosea* extract lowers glucose levels in *C. elegans* via activation of the AMPK signaling pathway (Teng et al., 2022).

In summary, this dissertation contributes both novel mechanistic insights into the effects of natural products on ageing processes and the development of an integrative experimental platform with broad research potential. The findings support the concept that targeting fundamental biological mechanisms of ageing with natural compounds represents a realistic and scientifically grounded strategy for extending healthspan, and they provide a foundation for future molecular and clinical research in the fields of gerontology and phytotherapy.

VII. FINDINGS

1. The model system *Caenorhabditis elegans* was successfully integrated as a platform for investigating the potential of plant-derived natural products to modulate ageing processes and regulate longevity at the organismal level.
2. Evidence was obtained for the hormetic properties of the prenylated flavonoid icariin, through which lifespan extension and stress response modulation are achieved.
3. Icariin exerts a geroprotective effect by modulating the daf-2 and hsf-1 signaling pathways, thereby attenuating age-associated physiological decline.
4. The extract of *P. granatum* improves mitochondrial function, delays ageing processes, and extends lifespan through the coordinated interaction of the transcription factors HLH-30, SKN-1, and DAF-16.
5. Pomegranate juice demonstrates potential to mitigate age-related physiological decline and improves functional parameters associated with healthy ageing.
6. The plant-based adaptogenic formulation ADAPT-232 enhances healthspan by modulating mitochondrial function and lipid homeostasis.

VIII. CONTRIBUTIONS

With scientific and fundamental character:

1. The effectiveness of *C. elegans* as an integrative model system for investigating natural products with the potential to modulate ageing and longevity at the organismal level has been demonstrated.
2. The hormetic nature and mechanism of action of icariin have been established, involving modulation of insulin/insulin-like signaling and hsf-1.
3. For the first time, the role of the transcription factor HLH-30 as a key mediator of the geroprotective effects of pomegranate leaf extract has been identified, acting in coordination with SKN-1 and DAF-16.
4. The effects of pomegranate juice on ageing-related physiological parameters in *C. elegans* have been characterized.
5. The potential of ADAPT-232 to modulate ageing processes through regulation of mitochondrial function and metabolic homeostasis has been demonstrated.

Scientific and applied contributions:

1. An integrated experimental platform for the functional evaluation of natural products with potential effects on ageing and longevity in *C. elegans* has been developed and implemented.
2. The obtained data on the geroprotective effects of ADAPT-232 provide a basis for its potential repositioning from a product used for stress and physical performance management to an intervention with possible applications in maintaining metabolic balance and mitochondrial health.
3. A model of mitochondrial dysfunction based on the induction of metabolic stress through high-carbohydrate exposure in *C. elegans* has been adapted and validated, enabling its use for the evaluation of metabolically targeted interventions.

Acknowledgements

I would like to express my deep gratitude to my supervisor, Prof. Milen I. Georgiev, for his trust, patience, inspiring ideas, and invaluable guidance throughout my doctoral studies.

I sincerely thank my colleagues from the Laboratory of Metabolomics at the Institute of Microbiology “Stefan Angelov”, Plovdiv, and from the Center of Plant Systems Biology and Biotechnology, Plovdiv, for their support, shared ideas, and the pleasure of conducting research together.

I extend my appreciation to the management of the Institute of Microbiology “Stephan Angeloff” for providing a stimulating research environment and opportunities for professional development.

The research presented in this dissertation was supported by the PlantaSYST project (SGA No. 739582 and FPA No. 664620) under the European Union’s Horizon 2020 programme, as well as by project BG05M2OP001-1.003-001-C01, funded by the European Regional Development Fund through the Operational Programme “Science and Education for Smart Growth”.

This work was also supported by the National Science Fund of the Ministry of Education and Science of the Republic of Bulgaria (grant agreements № КП-06-КОСТ/11 и № КП-06-КОСТ/12).

Publications related to the dissertation

Scientific publications

1. **Todorova M.N.**, Savova M.S., Mihaylova L.V., Georgiev M.I. (2024) Nurturing longevity through natural compounds: Where do we stand and where do we go? *Food Frontiers*, 5: 267-310 (**IF$_{2024}$ 6.9; Q1**).
2. **Todorova M.N.**, Savova M.S., Mihaylova L.V., Georgiev M.I. (2024) Icariin improves stress resistance and extends lifespan in *Caenorhabditis elegans* through *hsf-1* and *daf-2*-driven hormesis. *International Journal of Molecular Sciences*, 25(1): 352 (**IF$_{2024}$ 4.9; Q1**).
3. **Todorova M. N.**, Savova, M. S., Mihaylova, L. V., Georgiev M.I. (2024) *Punica granatum* L. leaf extract enhances stress tolerance and promotes healthy longevity through HLH-30/TFEB, DAF16/FOXO, and SKN1/NRF2 crosstalk in *Caenorhabditis elegans*. *Phytomedicine*, 134: 155971 (**IF$_{2024}$ 8.3; Q1**).

Participation in scientific forums

Oral reports

1. **Todorova M.N.**, Georgiev M.I. (2023) Targeting pro-longevity pathways in *Caenorhabditis elegans* through natural compounds – icariin effect on stress resistance and lifespan. *CIVIS BIP Program "From medicinal plants to drug products"*, 18 September – 06 October, Athens, Greece.
2. Georgiev M.I., **Todorova M.N.** (2024) Nurturing longevity through natural compounds. *12th Conference on Medicinal and Aromatic Plants of Southeast European Countries*, 17–19 October, Izmir, Turkiye.
3. Georgiev M.I., Mihaylova L.V., Savova M.S., **Todorova M.N.** (2024) Utilizing natural products for weight management and longevity promotion. *International Congress on Natural Products Research*, 13–17 July, Krakow, Poland.

Poster presentations

1. **Todorova M.N.**, Savova M.S., Mihaylova L.V., Georgiev M.I. (2023) Effect of icariin on longevity stress resistance and fitness of *Caenorhabditis elegans*. *5th International Conference of Natural Products Utilization: from Plants to Pharmacy Shelf*, 30 May – 2 June, Sts. Constantine and Helena resort, Bulgaria.
2. **Todorova M.N.**, Savova M.S., Mihaylova L.V., Georgiev M.I. (2023) Plant-derived

natural compounds for healthspan improvement and longevity. *2nd International Conference on Plant Systems Biology and Biotechnology*, 25–26 September, Center of Plant Systems Biology and Biotechnology, Plovdiv, Bulgaria.

3. **Todorova M.N.**, Binev B.K., Georgiev M.I. (2024) Exploring the potential of ADAPT-232: plant adaptogens for healthy aging, and longevity in *Caenorhabditis elegans*. *International Congress on Natural Products Research*, 13–17 July, Krakow, Poland.
4. **Todorova M.N.**, Savova M.S., Mihaylova L.V., Binev B.K., Georgiev M.I. (2024) Exploring the therapeutic potential of *Punica granatum* leaves extract in enhancing healthspan and lifespan in *Caenorhabditis elegans*. *International Congress on Natural Products Research*, 13–17 July, Krakow, Poland.

Citations of publications related to the dissertation, excluding self-citations – 17 (Scopus, 02.04.2026); H-index – 4.

Total impact factor of publications related to the dissertation – 20.1.